RNAi screening of RING/U-box domain ubiquitin ligases identifies critical regulators of stem cells and tissue regeneration in planarians

John M. Allen[1,2], Madison Balagtas[1], Elizabeth Barajas[1], Carolina Cano Macip[1], Sarai Alvarez Zepeda[1], Ionit Iberkleid[1], Elizabeth M. Duncan[2], and Ricardo M. Zayas[1]

[1]Department of Biology, San Diego State University, 5500 Campanile Dr., San Diego, CA 92182-4614, USA.

[2]Deparment of Biology, University of Kentucky, 101 T.H. Morgan Building, Lexington KY, 40506-022, USA.

***Correspondence should be addressed to:**
Dr. Ricardo M. Zayas
E-mail: rzayas@sdsu.edu

Short Title: "Planarian RING/U-box domain E3 ligases."

Keywords: Planarian, Stem Cells, Regeneration, E3 ubiquitin ligases, PRC1, Prpf19, RNF2

Abstract

Regenerative processes depend on the interpretation of signals to coordinate cell behaviors. The role of ubiquitin-mediated signaling in regeneration is not well understood. To investigate how ubiquitylation might specifically impact tissue regeneration, we are studying planarians that are capable of regenerating from nearly any injury using a population of stem cells. Here we used RNAi to screen RING/U-box E3 ubiquitin ligases that are highly expressed in planarian stem cells and stem cell progeny. RNAi screening identified nine genes with functions in regeneration, including the spliceosomal factor *prpf19* and epigenetic regulator *rnf2*; based on roles in developmental processes, we further explored these two genes. We found that *prpf19* was required for survival but not for stem cell maintenance, suggesting a role in promoting cell differentiation. Because RNF2 is the catalytic subunit of the Polycomb Repressive Complex 1 (PRC1), we also examined other cofactors of *rnf2* and observed a striking phenotype of regional tissue misspecification in *cbx* and *phc* RNAi planarians. To identify genes regulated by PRC1, we performed RNA-seq after knocking down *rnf2* or *phc* and found that the set of genes differentially expressed were largely non-overlapping despite being predicted to function in the same complex. Using *in situ* hybridization, we showed that *rnf2* regulates gene expression levels within a tissue type, whereas *phc* is necessary for the spatial restriction of gene expression. This work uncovered roles for RING/U-box E3 ligases in stem cell regulation and regeneration and identified differential gene targets for PRC1 factors required for maintaining cell-type-specific gene expression in planarians.

43 ## Introduction

44 A deep understanding of the networks and signaling pathways that direct the
45 maintenance and differentiation of adult stem cells is essential for regenerative
46 therapies. The freshwater planarian, *Schmidtea mediterranea*, is an important model for
47 studying the molecular mechanisms that underpin stem cell-based regeneration[1,2].
48 These worms maintain a large population of adult stem cells, a subset of which have
49 been demonstrated to be pluripotent[3,4]. This population of stem cells continuously
50 renews planarian tissues during homeostasis and is also mobilized in response to injury
51 to regenerate tissues[5,6]. As such, they offer an amenable model to study stem cell
52 biology in a whole-organism *in vivo* context.

53 Extensive work has been performed to understand the molecular basis of
54 planarian regeneration[7], yet most studies have primarily examined transcriptional
55 changes[8-12]. Comparatively, fewer studies have focused on proteomic regulation in
56 planarian stem cells[13,14] or the post-translational regulation of proteins vital for stem cell
57 function[15]. An essential post-translation regulator of proteins is the addition of the small,
58 highly conserved polypeptide ubiquitin, which modifies protein function in myriad cellular
59 contexts, including transcription, cell cycle regulation, translational fidelity, protein
60 turnover, and degradation[16-19].

61 Ubiquitin-dependent signaling events have emerged as essential regulators of
62 stem cell functions, including self-renewal and differentiation[20]. The transfer of free
63 ubiquitin onto a target substrate typically occurs through a tripartite enzymatic cascade
64 that terminates with the E3 ubiquitin ligases. The E3 ligases can be grouped into two

65 major classes, the HECT (Homologous to the E6-AP Carboxyl Terminus) and the more
66 prevalent RING (Really Interesting New Gene) class. Of the approximately 617 genes
67 encoding putative E3 ligases identified in the human genome, 309 were predicted to
68 contain a RING finger (RNF) or the related U-box domain; a further 270 E3 genes that
69 function in complexes associated with RINGs[21]. The RNFs are defined by a zinc-finger
70 domain with an evolutionarily conserved arrangement of cysteine and histidine residues
71 that coordinate two zinc ions and bind an E2-ubiquitin conjugate[22]. The U-box domain
72 forms a similar structure to the RING domain and can bind conjugated E2 but does not
73 coordinate zinc[23]. Substrate recognition and binding are achieved by additional domains
74 within the RNF protein or association with other proteins as part of a multi-protein
75 complex. Previous work on E3 ligase function in planarians has implicated HECT E3
76 and Cullin-Ring complex member ligases as essential regulators of regeneration and
77 stem cells[15,24].

78 Here we performed functional analysis on a subset of RING and U-box domain-
79 containing genes that are expressed in the planarian stem cells or progeny. We found
80 several to be essential for homeostatic maintenance, regeneration, and tissue
81 patterning. These genes included spliceosomal factor *prpf19* and epigenetic factors *rnf2*
82 and *bre1*, known to ubiquitylate histones. We found that *prpf19* was required for worm
83 survival but not for stem cell maintenance, suggesting a role in promoting cell
84 differentiation. Polycomb Repressive Complex 1 (PRC1) component gene *rnf2* was
85 required for global monoubiquitylation of histone H2A (H2Aub1) and promoting proper
86 regeneration. In addition, when we disrupted PRC1genes *phc* and *cbx*, we did not
87 observe a global reduction in H2Aub1 levels but did observe defects in the organization

88 of tissue near the base of the planarian pharynx. Taken together, analysis of RING/U-
89 box E3 ligases identified stem cell biology and regeneration regulators and led to
90 discovering differential phenotypes and transcriptional targets for PRC1 factors.

91

92

93 # Results

94 **Identification of RING and U-Box E3 ubiquitin ligase genes in *S. mediterranea***

95 The RING and U-Box protein domains have been identified as having a pivotal
96 role in mediating the ubiquitylation of a target substrate. To identify genes in *S.*
97 *mediterranea* that are predicted to encode a RING/U-box domain, we filtered a
98 reference planarian transcriptome[25] using InterPro domain annotations and generated a
99 list of 393 transcripts. Next, we used the predicted RING and U-box domain-containing
100 gene transcripts to perform BLAST analysis using a curated list of human E3 ubiquitin
101 ligases[21]. We found 376 planarian genes that were predicted to have homology with a
102 human RING/U-box gene (Supplemental Table S1) and 17 planarian transcripts that did
103 not have predicted significant homology to a human RING/U-box gene.

104

105 **A functional screen reveals genes with roles in planarian stem cell regulation and**
106 **regeneration**

107 To identify RING/U-box genes that regulate planarian stem cells and
108 regeneration, we assessed the function of 93 genes from our list, including 72
109 genes most highly expressed in stem cells or stem cell progeny[8] (Supplemental Table
110 S2). RNAi treatments were performed over the course of four weeks while the worms
111 were observed for defects in homeostasis. After 28 days, the worms were amputated to
112 assess the effect of RNAi treatment on regeneration (Figure 1A). We found that RNAi of
113 nine genes produced phenotypes related to stem cell function in homeostasis during
114 regeneration (Table 1). Phenotypes observed during homeostasis included head

115 regression, epidermal lesions, ventral curling, and lysis (Figure 1B); other genes
116 displayed abnormalities and delays during regeneration when disrupted (Figure 1C).
117 During homeostasis, head regression was observed after RNAi-mediated disruption of
118 *prpf19*, *march5*, *traf2-like*, *not4*, and *bre1*; lesions were observed after disruption of
119 *march5*, *ran*, and *rnf8-like*; and ventral curling was observed after disruption of *prpf19*
120 and *not4*. The genes *prpf19*, *march5*, and *ran* were essential for worm survival, and
121 depletion of these genes caused worm lysis. Knockdown of *rnf8-like*, *bre1*, *rnf2*, and
122 *ring1* caused defective regeneration, typically manifested as a delayed appearance of
123 visible eyespots compared to *control(RNAi)* treatments. We chose to characterize a
124 subset of these phenotypes further based on their strong expression in stem cells
125 (Supplemental Figure S1B) or known roles as epigenetic regulators of stem cells during
126 developmental processes.

127

128 **Spliceosomal factor *prpf19* is required for worm survival and stem cell function**

129 The U-box gene *prpf19* had enriched expression in planarian stem cells, and our
130 initial screen revealed that its expression was required for worm survival. Other aspects
131 of the RNAi phenotype, including head regression and ventral curling, are typically
132 associated with depletion or loss of stem cells in planarians. These phenotypes are
133 consistent with an earlier report for *prpf19* as being up-regulated during, and necessary
134 for, head regeneration in planarians[26]. *prpf19* is a member of NineTeen Complex (NTC),
135 with a well-described role in regulating mRNA splicing that is conserved in
136 *Saccharomyces cerevisiae*. Consistent with a role in an essential cellular process, we
137 found broad expression of this gene using WISH (Supplemental Figure S1A).

138 Furthermore, we found that at least a subset of this expression is in the stem cells or
139 stem cell progeny by performing WISH of irradiated worms (Supplemental Figure S1B).
140 We confirmed this observation using double fluorescent in situ hybridization (FISH) to
141 observe co-expression of *prpf19* with stem cell markers *piwi-1* and *h2b*, and stem cell
142 progeny markers *prog-1* and *agat*-1 (Supplemental Figure S2A-B). As *prpf19* is known
143 to function as an E3 ubiquitin ligase, we assayed the effect of *prpf19* inhibition on
144 ubiquitylated proteins by western blotting and found no noticeable difference with
145 control samples (Supplemental Figure S2C), suggesting that *prpf19(RNAi)* does not
146 have an appreciable effect on general proteasome function but rather or has only a
147 minor effect on global ubiquitylation or is targeting specific proteins that are not
148 resolvable on a total ubiquitin blot.

149 To investigate if the *prpf19(RNAi)* phenotypes observed were the result of stem
150 cell depletion, we performed WISH to planarian stem cell marker genes *tgs-1*, *piwi-1,*
151 and *h2b*, on *prpf19(RNAi)* and control worms. Surprisingly, all marker genes analyzed
152 showed robust expression, even in worms where the phenotype had significantly
153 progressed (Figure 2A). Because *prpf19* was found to be expressed in additional cell
154 types besides stem cells (Supplemental Figure S2B), we also examined the effect of
155 *prpf19* inhibition on epidermal progeny by performing WISH with markers for early and
156 late epidermal progeny, *prog-1* and *agat-1*, respectively[10,27]. Consistent with the
157 epidermal lesions observed during the progression of the *prpf19* phenotype, staining for
158 epidermal lineage markers was reduced in *prpf19(RNAi)* worms. These results suggest
159 that *prpf19* function is not required for the maintenance and survival of planarian stem

160 cells but may affect the differentiation of stem cells into progenitors or the maintenance
161 of progenitor populations.

162

163 **Inhibition of *prpf19* causes defects in stem cell proliferation and increases**
164 **apoptosis**

165 Despite being dispensable for stem cell maintenance, the strong expression of
166 *prpf19* in stem cells and robust phenotypes that resulted from *prpf19* inhibition
167 suggested a role for *prpf19* in regulating stem cell dynamics. To examine the effect of
168 *prpf19* RNAi on cell proliferation, we stained *control(RNAi)* and *prpf19(RNAi)* treated
169 worms with anti-phospho-histone H3 (pH3) to mark mitotic cells across several time
170 points of treatment. We found that at late time points (day 18), when the phenotype is
171 beginning to manifest, there was a significant decrease in the number of mitotic cells in
172 *prpf19(RNAi)* worms (Figure 2B and 2C). This decrease in the number of mitotic cells
173 was not correlated with a reduction in the expression of stem cell marker genes (Figure
174 2A, Supplemental Figure S2A), suggesting that *prpf19(RNAi)* treatment blocks or alters
175 the rate of stem cell differentiation.

176 To better understand the severe phenotypes observed in *prpf19(RNAi)* worms, including
177 epidermal lesioning and worm lysis, we assayed the worms for apoptotic cells. Not
178 surprisingly, we found an increase in apoptotic cells in *prpf19(RNAi)*-treated worms
179 compared to control worms at the time point before observing phenotypes, and a
180 marked increase was observed as the *prp19f(RNAi)* phenotype progressed (Figure 2D
181 and 2E). This result is congruous with reports of *prpf19* having anti-apoptotic effects in

182 human cell lines[28]. Together with the observed loss of epidermal progenitor markers
183 (Figure 2A), these data suggest that the phenotypes observed after *prpf19* depletion are
184 not caused by a loss of stem cells but rather by dysfunction in the proper homeostatic
185 replacement of differentiated tissues. After *prpf19* disruption, stem cells are unable to
186 replenish tissues, either through impaired differentiation or reduced proliferation, and
187 epidermal integrity becomes compromised. In addition, there could also be a role for
188 *prpf19* as an antiapoptotic factor in differentiated tissues, resulting in increased
189 apoptosis in *prpf19(RNAi)* worms.

190

191 **NTC components and targets are necessary for tissue renewal and regeneration**

192 NTC is a large protein complex with various cellular roles but has its best-
193 described role in regulating pre-mRNA splicing. Named after its founding member,
194 *prpf19*, the complex is conserved between humans and yeast. In the spliceosome, NTC
195 functions as an E3 ligase through its PRPF19 subunit (Figure 3A). To examine if the
196 effects of *prpf19* RNAi were being mediated through disruption of spliceosomal
197 assembly and function, we knocked down three homologs of core NTC component
198 members, *cdc5l*, *prlg1*, and *spf27* (Supplemental Table S3). We found that these genes
199 were also necessary for worm survival and regeneration (Figure 3B and 3C). *cdc5l* and
200 *prlg1* are essential for NTC function in yeast and presented very severe phenotypes of
201 head regression, ventral curling, and lysis that mirrored the observations for
202 *prpf19(RNAi)*. *Spf27(RNAi)* worms displayed a milder phenotype than other NTC genes
203 examined and showed delayed or absent regeneration in 28/37 head fragments and
204 33/37 trunk fragments; an additional three trunk fragments showed a more severe

205 phenotype of ventral curling and lysis. Also, we postulated that if the *prpf19* RNAi
206 phenotype resulted from its ubiquityl ligase activity within the NTC complex, inhibiting
207 *prpf3* or *prpf8* should result in a similar phenotype. Indeed, we found that *prpf3(RNAi)*
208 and *prpf8(RNAi)* worms exhibited severe phenotypes like *prpf19(RNAi)*, including head
209 regression, ventral curling, epidermal lesions, and lysis (Figure 3D). WISH analysis of
210 NTC genes, *prpf3* and *prpf8*, demonstrated broad parenchymal expression patterns like
211 *prpf19*, with *prpf8* showing a noticeable stem cell expression pattern (Supplemental
212 Figure S3A). The similar phenotypes and expression patterns observed for NTC genes
213 and factors downstream to *prpf19* suggested that the *prpf19(RNAi)* phenotype is
214 mediated through its role in NTC and that the NTC and spliceosome function is critical
215 for stem cell regulation during homeostasis and regeneration.

216

217 **Histone-modifying ubiquitin ligases are essential for regeneration and**
218 **homeostasis**

219 Ubiquitylation of histone H2B is associated with transcriptional activation and is
220 mediated by the E3 ligase complex RNF20/40 (Bre1 in yeast)[29,30]. We found that
221 planarians have a single homolog for this complex named *Smed-bre1* (referred to as
222 *bre1* hereon), and that knockdown of *bre1* caused the worms to exhibit head regression
223 and lesions prior to day 28 of treatment in 33/53 worms assayed (Figure 1B).
224 Furthermore, most *bre1(RNAi)* worms failed to regenerate when amputated, and many
225 lysed with 31/53 head fragments and 21/53 trunk fragments lysing by the end of the
226 observation period (day 14 post-amputation). To investigate if *bre1(RNAi)* affected
227 global levels of monoubiquityl-histone H2B (H2Bu1), we performed a protein blot using

228 an H2Bub1-specific antibody. We found reduced levels of H2Bu1 in whole worm
229 homogenates as soon as 14 days after beginning RNAi treatment (Supplemental Figure
230 S4A).

231 In contrast to histone H2B ubiquitylation, monoubiquitylation of histone H2A is
232 associated with transcriptional repression. It occurs in various cellular contexts,
233 including developmental processes, stem cell regulation, and the DNA damage
234 response. Histone H2A is targeted for ubiquitylation by RING1 and RNF2, which act as
235 RING E3 ligases within PRC1. PRC1 is a repressive epigenetic complex active during
236 development to monoubiquitylate histone H2A[31] and stably silence genes[32] (Figure 4A).
237 We identified two candidate homologs of RING1 and RNF2 and found that depletion of
238 each caused delayed or absent regeneration compared to controls. These phenotypes
239 were most evident in the trunk fragments where 37/58 *rnf2(RNAi)* and 19/29
240 *ring1(RNAi)* worms exhibited a delayed regeneration phenotype (measured by the
241 appearance of dark eyespots) compared to 7/54 and 2/30 *control(RNAi)* worms assayed
242 at the same regeneration time point (7 days post-amputation). Of the 37/58 *rnf2(RNAi)*
243 trunks and 19/29 *ring1(RNAi)* trunks with regeneration defects, 13/37 and 4/19 failed to
244 form regeneration blastemas, respectively, whereas all *control(RNAi)* worms formed
245 normal-sized blastemas (Figure 1C). No obvious phenotypes were observed during
246 homeostatic maintenance, even during long-term RNAi treatment (>16 feeds over eight
247 weeks). To assess if the ubiquityl ligase activity of *rnf2* towards histone H2A was
248 conserved in planarians, we examined bulk levels of H2Aub1 by protein blot analysis
249 using an H2Aub1 specific antibody and observed markedly reduced levels of H2Aub1
250 after *rnf2* inhibition (Figure 4B). In contrast, we found that *ring1* RNAi did not

251 appreciably affect global H2Aub1 levels (Supplemental Figure S4B), consistent with *rnf2*
252 being the E3 ligase subunit within PRC1 that is responsible for H2A ubiquitylation[31,33].

253

254 **Disruption of canonical PRC1 subunit *phc* affects the patterning of the planarian**
255 **pharyngeal body region**

256 To gain insight into the role of PRC1 in planarians, we examined the functional
257 requirements for PRC1 subunits. In vertebrates, the composition of PRC1 is variable[34];
258 the complex is defined by which of the six mammalian paralogs of PGCF is present.
259 PCGF2 and PCGF4 define the mammalian canonical PRC1 complex (cPRC1), which
260 also includes one each of several chromobox (CBX) and Polyhomeotic (PHC) paralogs
261 (Figure 4A). We identified planarian homologs for these other core PRC1 genes and
262 found a single homolog for *cbx* and *phc* and two homologs for *pcgf* (Supplemental Table
263 S3). To investigate if the phenotypes for *rnf2(RNAi)* and *ring1(RNAi)* were mediated
264 through their function in canonical PRC1, we used RNAi to deplete *cbx*, *phc*, *pcgf2*, and
265 *pcgf3*.

266 In contrast to the impaired regeneration observed after *rnf2* or *ring1* knockdown,
267 RNAi for *phc* or *cbx* demonstrated a complex homeostasis phenotype that included the
268 abnormal appearance of a dorsal lesion anterior to the pharynx (Figure 4C). In some
269 cases, we observed the pharynx protruding from the lesioned region and extending
270 ectopically from the dorsal surface of the worm. As the phenotypes progressed, these
271 RNAi worms began to exhibit defects along the body axis, showing crimped tails unable
272 to affix to the dish and epidermal lesions. We also assayed the effect of inhibition of the

273 canonical PRC1 genes on H2Aub1 levels. We found that inhibition of *phc* or *cbx* did not
274 impact bulk H2Aub1 levels (Supplemental Figure S4B), suggesting that cPRC1 is not
275 responsible for most H2Aub1 deposition, like findings in vertebrate models[35]. Both *phc*
276 and *cbx* had similar mRNA expression patterns, suggesting that they can function in the
277 same complex (Supplemental Figure S4C). This expression pattern overlapped with the
278 diffuse parenchymal expression pattern for *rnf2* and *ring1* (Supplemental Figure S1A)
279 but had more robust expression near the planarian brain and intestinal branches, the
280 latter of which are areas known to be enriched in stem cells.

281 While similar, the penetrance of the *phc(RNAi)* phenotype was higher than for
282 *cbx(RNAi),* and we chose to examine the *phc(RNAi)* phenotype further using known
283 markers of tissue patterning. The appearance of a dorsal lesion and mislocalization of
284 the pharynx to the dorsal surface in *phc(RNAi)* animals suggests that planarian PRC1
285 may be involved in the specification of specific tissues related to the pharynx or in
286 regulating genes that provide axial positioning cues to stem cell progeny during
287 homeostatic tissue turnover. We examined dorsal-ventral patterning factor *bmp-4*[36] and
288 anterior-posterior factor *ndl-3*[37] expression after *phc(RNAi)* and did not observe a
289 noticeable change in the expression pattern of these factors relative to controls
290 (Supplemental Figure S4D). We then further examined genes that mark specific tissues
291 related to the pharynx, including the pharynx marker *laminin*[38] and the gene *NB.22.1E*[39],
292 which labels marginal adhesive gland cells, the ventral mouth opening, and a population
293 of cells near the base of the pharynx. Following *phc* inhibition, we observed that *laminin*
294 expression was reduced to a single condensed spot of expression near the location of
295 the dorsal lesion and a few scattered cells near the midline (Figure 4D). Likewise, we

296 observed the specific disappearance of the *NB.22.1E*$^{+}$ population of cells at the base of
297 the pharynx following *phc(RNAi)*. In contrast, expression along the body margin and
298 ventral mouth opening was unaffected (Figure 4D). These data establish a role for
299 PRC1 factors in maintaining tissue identity in a non-embryological context.

300

301 **RNA-seq analysis of gene expression after PRC1 subunit inhibition reveals**
302 **candidate transcriptional targets of PRC1**

303 To investigate which genes are differentially expressed after PRC1 inhibition and
304 to understand the transcriptional basis for the *rnf2* and *phc* RNAi phenotypes, we
305 performed RNA-seq. We chose time points based on the phenotypic progression,
306 quantitative PCR analysis to confirm a robust reduction in target RNAi transcript levels
307 (not shown), and, for *rnf2(RNAi)*, protein blot analysis to ensure the RNAi treatment was
308 reducing levels of H2Aub1. Based on these parameters, we extracted RNA after 11
309 days of *phc* RNAi treatment and 14 and 28 days after *rnf2* RNAi (Supplemental Figure
310 S5A). For *rnf2(RNAi)*, we identified 264 differentially expressed genes (126 down-
311 regulated and 138 up-regulated) (Figure 5A, Supplemental Figure S5B). Not
312 surprisingly, an extended *rnf2* RNAi treatment increased the number of differentially
313 expressed genes: 247 genes were differentially expressed after 28 days compared to
314 29 after 14 days of treatment (Table 2). Also, there was substantial overlap between the
315 *rnf2(RNAi)* data sets, with 12 of 29 genes in the day 14 data set represented in the day
316 28 data set (Supplemental Figure S5C). After 11 days of *phc(RNAi)*, 49 genes were
317 differentially expressed: 20 were down-regulated and 29 up-regulated (Figure 5C).
318 Consistent with a repressive role in transcriptional regulation, more genes were

319 significantly up-regulated when either *phc* or *rnf2* was inhibited. Importantly, *rnf2* and
320 *phc* were each significantly down-regulated when targeted for RNAi.

321 Surprisingly, despite being predicted to function in a complex together, only a
322 single gene was found in common between the *phc(RNAi)* and *rnf2(RNAi)* data sets.
323 Intriguingly, this gene was *cbx*, which encodes a chromatin-binding element within
324 PRC1, and was the most significantly up-regulated gene after *phc* knockdown. This
325 overall lack of overlap between the data sets suggests that *phc* and *rnf2* regulate
326 different processes and pathways *in vivo,* and this difference explains the disparate
327 phenotypes observed after RNAi treatment.

328 To gain insight into the RNA-seq data set, we performed Gene Ontology (GO)
329 analysis on the differentially expressed gene set from the day 28 *rnf2(RNAi)* gene set.
330 The down-regulated genes were significantly enriched for GO biological process terms
331 related to metabolic and catabolic processes (Supplemental Figure S5D). Conversely,
332 among GO terms enriched in up-regulated genes were cellular stress (Supplemental
333 Figure S5E), especially low oxygen conditions, including "response to hypoxia"
334 (GO:0001666), "cellular response to decreased oxygen levels" (GO:0036294), "ATF6-
335 mediated unfolded protein response" (GO:0036500), "regulation of transcription from
336 RNA polymerase II promoter in response to stress" (GO:0043618), "chaperone
337 cofactor-dependent protein refolding" (GO:0051085), "protein folding in endoplasmic
338 reticulum" (GO:0034975), and "protein refolding" (GO:0042026). These GO annotations
339 suggest that *rnf2* activity represses cellular responses to stress during normal
340 homeostatic conditions and that epigenetic mechanisms facilitate the switch between
341 homeostasis and cellular stress responses.

342 To investigate the spatial expression changes of differentially expressed genes
343 from our RNA-seq data sets, we selected a subset to examine using WISH after *phc* or
344 *rnf2* RNAi (Supplemental Table S4). For *rnf2(RNAi)*, we selected 33 differentially
345 expressed genes that were predicted to be involved in the extracellular matrix, stress
346 response factors, cell signaling, and chromatin regulation or transcription and assayed
347 their expression after *rnf2* depletion. In general, *rnf2(RNAi)* caused a subtle effect on
348 gene expression levels. However, in some instances, a robust change in expression
349 occurred in *rnf2(RNAi)* worms, as seen clearly for *Smed-colec10* and *Smed-colec11*;
350 expression of these genes is nearly undetectable in control worms as compared to
351 *rnf2(RNAi)* worms (Figure 5B). Taken together, the GO and *in situ* analyses indicate
352 that *rnf2* functions in broad cellular processes and that it maintains gene expression in
353 differentiated tissues at appropriate levels.

354 In contrast to the mild effect on gene expression observed in *rnf2(RNAi)* animals,
355 assaying mRNA expression of putative PHC target genes revealed striking changes in
356 expression levels and spatial patterning in *phc(RNAi)* worms. We examined 11 genes
357 using *in situ* hybridization, including genes involved in cell adhesion, cell signaling,
358 transcription, and chromatin regulation. For 7 of these 11 genes, strong ectopic
359 expression was observed in *phc(RNAi)* worms in the region of the worm where the
360 dorsal lesion forms (Figure 5D). Genes ectopically expressed in this region included the
361 cell adhesion factor *icam5*, the Cut homeobox transcription factor *onecut1*, and *roar*,
362 which encodes an orphan nuclear receptor. We also found several chromatin regulators
363 that were misexpressed in the region near the pharynx, including *cbx*, *pc-like*, *smc4*,
364 and *kat6a*. Additionally, we found that the extracellular matrix protein *egflam*, which is

365 normally expressed in the nervous system and pharynx tip, was significantly down-
366 regulated throughout the worm.

367 The ectopic expression of specific factors and disruption of *NB.22.1E* and
368 *laminin* expression at the site of tissue defects in *phc(RNAi)* worms indicates that *phc*
369 function is required to maintain the proper specification and integrity of tissues in this
370 region.

371

372 ## Discussion

373 To address the role of ubiquitin signaling in stem cell regulation and regeneration
374 in a whole organism *in vivo* context, we performed a functional screen of the RING/U-
375 box class of E3 ubiquitin ligases that are expressed in stem cells and progeny in *S.*
376 *mediterranea*. The screen identified nine genes that demonstrated phenotypes related
377 to stem cell function or regeneration, building on previous studies from our lab on the
378 HECT[24] and Cullin[15] classes of E3 ligases.

379 A U-box gene that we chose to investigate in further detail was *prpf19*, the
380 founding member of the large protein complex NTC. First characterized in yeast, the
381 best described role for NTC is in the spliceosome, where the E3 ligase function of
382 Prpf19 is essential for forming snRNP conformations[40]. We found that depletion of
383 *prpf19* caused a strong homeostasis phenotype that included head regression,
384 lesioning, ventral curling, and lysis, all of which are morphological effects often caused
385 by stem cell depletion. We depleted other NTC member genes in this study and
386 observed similar phenotypes to *prpf19(RNAi)*, suggesting that the *prpf19(RNAi)*
387 phenotype is mediated through its role in NTC. In addition, we found that the stem cell
388 population was maintained in *prpf19(RNAi)* worms, suggesting an alternative
389 mechanism of dysregulation. Our results are consistent with a previous study that
390 observed a similar phenotype upon depletion of *prp19,* which showed an effect on head
391 regeneration without disrupting the stem cells[26].

392 Post-transcriptional processing of RNAs is emerging as a major regulator of
393 planarian stem cells and differentiation. The PIWI homolog *smedwi-2* was identified as

394 nonessential for stem cell maintenance but necessary for proper differentiation[41], and
395 *smedwi-3* was shown to regulate stem cell mRNAs through two distinct activities[42]. A
396 screen of planarian ribonucleoprotein granule component homolog genes demonstrated
397 that most were expressed in planarian stem cells and that depletion of several genes,
398 including mRNA turnover factors, exoribonucleases, and DEAD-box RNA helicases,
399 inhibited regeneration without affecting proliferation or stem cell maintenance[43].
400 Similarly, the CCR4-NOT complex regulates the post-translational degradation of
401 mRNAs and has been shown to have a critical role in planarian stem cell biology[44]. The
402 phenotype of CCR4-NOT complex member gene *Smed-not1* was reported to have a
403 similar phenotype to *prpf19*, where the animals maintained proliferative stem cells
404 despite presenting a phenotypic that suggests loss of tissue renewal[44]. This study found
405 that an additional CCR4-NOT subunit, *not4*, is critical for worm homeostasis and causes
406 head regression and ventral curling upon inhibition (Figure 1B). This phenotype is
407 consistent with that of *not1(RNAi)*; however, in the future, it will be necessary to
408 examine the stem cell population using marker genes in *not4(RNAi)* worms to resolve if
409 the phenotype is mediated through a similar mechanism. Regulation of mRNAs in
410 planarian stem cells by several pathways, including piRNAs, deadenylation, or splicing,
411 is crucial for homeostasis and regeneration while being dispensable for stem cell
412 maintenance. These studies implicate post-transcriptional regulation of mRNAs in
413 planarian stem cells as a critical process for regulating differentiation.

414 Epigenetic regulation of gene expression is essential during development and
415 throughout organismal life. Our RNAi screen uncovered planarian homologs of histone-
416 targeting RING E3 ubiquitin ligases that affected worm homeostasis and regeneration

417 and confirmed that inhibition of *bre1* and *rnf2* reduced levels of monoubiquityl-histone
418 H2B and H2A, respectively. This work demonstrates that activating and repressive
419 signals provided through histone modifiers are essential for the proper specification of
420 stem cells and establishing cellular identity during regenerative events.

421 PRC1 is a major repressive complex that works during development to
422 ubiquitylate histone H2A, compact chromatin, and silence target gene expression[31,45-49].
423 PRC1 function was first discovered and was best characterized as a repressor of the
424 HOX genes during development[50]. The core PRC1 complex is defined by a RING and
425 PCGF protein that forms canonical (cPRC1) or variant PRC1 (vPRC1) depending on the
426 presence of additional factors[51]. The RING subunit acts as an E3 ligase that targets
427 histone H2A, and in vertebrates is either RING1 or RNF2[52]. In contrast to *Drosophila*,
428 we found that planarians have two homologs of RING1 and RNF2. While these are
429 likely to be lineage-specific paralogs instead of direct homologs of each vertebrate
430 gene, we find that, as in vertebrates, the *S. mediterranea rnf2* paralog acts as the major
431 ligase and is responsible for the bulk of histone H2A ubiquitylation. We did not observe
432 a noticeable difference in global H2Aub1 levels after *Smed-ring1* inhibition
433 (Supplemental Figure S4B). However, as both genes demonstrated similar
434 regeneration-specific phenotypes, they may share common targets or pathways.

435 In contrast to *rnf2(RNAi)*, when we perturbed other cPRC1 core elements *phc*
436 and *cbx*, we did not see a reduction in bulk H2Aub1 levels by western blotting. Work in
437 mammalian cell lines has determined that vPRC1 activity is responsible for most H2A
438 ubiquitylation with a minimal contribution from cPRC1 complexes[35,53]. Invertebrates
439 were not thought to contain vPRC1, but more recent phylogenic analysis that included a

440 greater variety of invertebrate model organisms indicates that vPRC1 likely evolved as
441 early as cnidarians[54]. Our protein blot results show a minimal contribution of cPRC1
442 genes *cbx* and *phc* to overall H2Aub1 levels *in vivo,* and the presence of two *S.*
443 *mediterranea pcgf* genes support the existence of vPRC1 in *S. mediterranea*.

444 To gain insight into which genes are regulated by *rnf2* and *phc,* we performed
445 RNA-seq following RNAi. Consistent with predicted roles in transcriptional repression,
446 inhibiting the function of either gene led to more up-regulated than down-regulated
447 differentially expressed genes. The only gene shared between the data sets was the
448 significantly up-regulated factor *cbx*. Thus, it is possible that cPRC1 autoregulates its
449 expression in planarians and that the disruption to chromatin homeostasis induced by
450 cPRC1 disruption causes a compensatory response involving other chromatin factors.

451 Using GO analysis, we found that *rnf2* regulates genes related to the cellular
452 stress response, and when we examined the expression of candidate genes from our
453 RNA-seq data set using WISH, we observed that gene expression changes in
454 *rnf2(RNAi)* animals occurred mainly within the endogenous expression pattern. These
455 data support a role for RNF2 and potentially H2A ubiquitylation, in tuning transcription
456 levels within a particular cell type, especially for pathways that are adaptive and
457 responsive to stressful stimuli.

458 In contrast to *rnf2(RNAi)*, we saw dramatic shifts in the spatial expression of
459 specific genes after *phc(RNAi)*, including several genes that showed ectopic expression
460 near the base of the pharynx where lesions formed in *phc(RNAi)* planarians. In this
461 affected region, we observed both up- (*intercellular adhesion molecule 5*) and down-
462 regulation (*pikachurin*) of genes that encode extracellular matrix and intercellular

463 adhesion molecules, suggesting that their dysregulation is likely linked to the formation
464 of the dorsal lesion seen after *phc* RNAi. The ectopically expressed genes also included
465 regulators of cellular specification, including nuclear receptors, transcription factors, and
466 chromatin modifiers. One gene we identified as being misexpressed after *phc* depletion
467 was that encoding the nuclear factor *onecut1*, a CUT, and homeobox domain-containing
468 transcription factor that promotes hepatocyte proliferation remodels chromatin
469 accessibility and promotes tumor growth in colorectal cancers[55-57]. Based on its role in
470 regulating transcription and tissue identity in other animal models, we suspect it may be
471 contributing to the change in patterning near the pharynx. Future investigation into this
472 factor will elucidate if *onecut1* misexpression drives regional tissue misspecification and
473 if inhibition of *onecut1* suppresses the *phc(RNAi)* phenotype.

474 PRC1 regulates gene expression through the post-translational ubiquitylation of
475 histone H2A and by compacting chromatin. A deeper understanding of the role of this
476 complex in regulating regeneration will require uncovering which genomic elements it
477 targets. In the future, assays like ChIP-seq[58] or Cut&Run[59] could be used to identify the
478 localization of H2Aub1 in the planarian genome to inform how genes are regulated
479 epigenetically to promote a robust regenerative response during injury and tissue re-
480 specification and remodeling.

481

482 # Methods

483 **Planarian care**

484 A clonal line of asexual *S. mediterranea* (CIW4) was used in all experiments and kept in
485 1X Montjuïc salts (1.6 mM NaCl, 1.0 mM $CaCl_2$, 1.0 mM $MgSO_4$, 0.1 mM $MgCl_2$, 0.1 mM
486 KCl, 1.2 mM $NaHCO_3$, pH 7.0) in food-grade plastic containers at 20°C[60]. Animals
487 selected for experiments were 3-6 mm in length and starved for one week before
488 experimentation.

489

490 **Gene identification and Cloning**

491 To find RING and U-box domain-containing genes in *S. mediterranea,* we filtered the
492 Dresden transcriptome[25,61] using InterPro Domain IDs[62], IPR001841 (Zinc finger, RING-
493 type), and IPR003613 (U box domain). This list was filtered to include only the longest
494 gene contig for each hit and was used as query sequences for a BLAST search to a
495 curated list of human RING and U-box genes[21] at an expected value cut-off of 10^{-3}. We
496 additionally filtered the Dresden transcriptome for contigs annotated with IPR013083
497 (Zinc finger, RING/FYVE/PHD-type). This list was filtered to remove duplicate entries,
498 and a BLAST search was performed against our list of human RING and U-box genes.
499 As the IPR013083 family contains non-RING and U-box genes, only genes that had
500 predicted homology to a human gene at an expected cut-off of 10^{-3} were appended to
501 our initial list. The sequences of interest were obtained from either an EST library[63] or
502 cloned using gene-specific primers into pPR-T4P using ligation independent cloning[64,65].

503 EST clone accession numbers and the primer sequences used are listed in
504 Supplemental Tables S2-S4.

505

506 **RNA interference**

507 During the initial screening, animals were fed double-stranded RNA (dsRNA) mixed with
508 a ≈3:1 mixture of liver-water paste twice per week for eight feeds and were amputated
509 pre-pharyngeally on day 28 of treatment to observe regeneration. *In vitro* transcribed
510 and dsRNA expressed in bacteria were used to perform RNAi during the initial
511 screening of RING and U-box genes; all subsequent RNAi knockdowns were performed
512 using bacterially-expressed dsRNA. *In vitro* dsRNA was synthesized as previously
513 described[66]; the entire reaction mixture was separated into eight aliquots, mixed with
514 liver paste, and stored until feeding. Bacterially expressed dsRNA was prepared by
515 growing cultures of *E. coli* strain HT115 transformed with the pPR-T4P plasmid[64,65]
516 containing the gene of interest and inducing dsRNA expression using IPTG. Bacteria
517 pellets were purified using centrifugation and mixed with liver paste for administration to
518 animals[67].

519

520 **In situ hybridization**

521 Antisense probes for *in situ* hybridization were synthesized as previously described[68]
522 from DNA templates amplified from pBS II SK(+) (Stratagene) or pPR-T4P[64,65] plasmid
523 vectors incorporating either digoxigenin or FITC labeled UTPs. Animals for whole-mount
524 in situ hybridization (WISH) were processed and hybridized as outlined previously[69].

525 Briefly, samples were sacrificed in 5% *n*-acetyl cysteine, fixed in 4% formaldehyde, and
526 bleached in a formamide/hydrogen peroxide bleaching solution. Samples were pre-
527 hybridized for two hours and then hybridized with probe overnight at 56°C. Next,
528 samples were incubated with an appropriate antibody, depending on the probe label
529 and subsequent development strategy. For chromogenic development, samples were
530 incubated with an anti-digoxigenin-AP antibody (Roche, 1:2000) and developed with
531 NBT/BCIP in AP buffer. Fluorescent *in situ* development was performed using Fast Blue
532 salts[70] or Tyramide Signal Amplification (TSA) after incubation with anti-digoxigenin-AP
533 or anti-FITC-POD (Roche, 1:300) antibodies, respectively, following previously
534 described protocols[69,71]. For irradiation experiments to eliminate dividing cells, worms
535 were exposed to 60 Gy of X-ray irradiation in a Precision CellRad Irradiation System
536 and processed for WISH 7 days post-irradiation.

537

538 **Anti-phosphohistone H3 immunohistochemistry**

539 Animals were incubated in ice-cold 2% hydrochloric acid for 5 minutes and fixed for 2
540 hours in Carnoy's solution at 4°C. Samples were washed in methanol for 1 hour at 4°C
541 and bleached overnight in 6% H_2O_2 diluted in methanol at room temperature. Animals
542 were washed out of methanol and into PBS-Tx and blocked in 1% Bovine serum
543 albumin (BSA) diluted in PBS-Tx for 4 hours at room temperature. Samples were
544 incubated with anti-phosphohistone H3 (Ser 10) (Cell Signaling 3377, 1:1000) diluted in
545 1% BSA/PBS-Tx overnight at 4°C. Antibody was developed using TSA as previously
546 described[69].

547

548 **TUNEL staining**

549 The Terminal Deoxynucleotidyl Transferase-mediated deoxyuridine triphosphate Nick
550 End-labeling (TUNEL) assay was performed to quantify apoptotic cells. Animals were
551 incubated in 5% *n*-acetyl cysteine (diluted in PBS) for 5 minutes and fixed in 4%
552 formaldehyde (diluted in PBS-Tx [PBS with 0.3% Triton X-100]) for 15 minutes.
553 Samples were then permeabilized in 1% SDS (diluted in PBS) and bleached overnight
554 in 6% H_2O_2 (diluted in PBS-Tx). Samples were then rinsed and stained using the
555 Apoptag Kit (Millipore-Sigma) as previously described[72].

556

557 **Protein extraction and western blotting**

558 Protein samples from RNAi worms were homogenized in Trizol and extracted from the
559 organic phase following the manufacturer-provided protocol with a modified
560 solubilization buffer (4M Urea, 0.5% SDS) and added sonication step of 10 one-second
561 pulses that were performed to increase protein recovery[73,74]. Samples were loaded onto
562 AnyKD TGX gels (BioRad), transferred using the semidry method to a 0.45m PVDF
563 membrane, and blocked in 5% nonfat milk/TBS-Tw (Tris-buffered saline with 0.1%
564 Tween-20). Antibodies to monoubiquityl-Histone H2A (Cell Signaling 8240) and
565 monoubiquityl-Histone H2B (Cell Signaling 5546) were diluted in 5% bovine serum
566 albumin in TBS-Tw at 1:2000 and 1:1000 respectively and incubated overnight at 4°C.
567 Washes were performed with TBS-Tw and anti-rabbit-HRP (Cell Signaling 7074) was
568 diluted in 5% nonfat milk/TBS-Tw at 1:2500 and incubated for 1 hour at room

569 temperature. Signal was developed using BioRad Clarity Western ECL Substrate
570 (BioRad 1705061).

571

572 **RNA sequencing**

573 Worms from three independent control and experimental RNAi groups per time
574 point were homogenized in Trizol, and RNA was extracted and purified following
575 manufacturer protocol. RNA was treated with the Turbo DNA-free kit and column
576 purified using the Qiagen RNeasy MinElute Cleanup kit. Three independent biological
577 groups were collected at each time point assayed for both control and experimental
578 (*rnf2* or *phc*) RNAi treatments. Samples were sequenced on an Illumina HiSeq 4000 to
579 a read depth of at least 15 million 150 bp paired-end reads. The sequenced reads were
580 submitted to the NCBI BioProject PRJNA768725. Reads were pseudoaligned to the
581 Dresden (dd_Smed_v6) transcriptome using kallisto[75], and differential gene expression
582 analysis was performed using the R Bioconductor package[76] and DESeq2[77] with an
583 FDR cut-off value of ≤ 0.1 applied. To perform Gene Ontology (GO) analysis,
584 differentially expressed transcripts from the day 28 *rnf2(RNAi)* data set were compared
585 to the human proteome using BLASTX (cut-off e-value < $1e^{-3}$). Human UniProt IDs were
586 used as input for annotation and overrepresentation analysis (http://geneontology.org/)
587 using Fisher's Exact test with an FDR multiple comparisons correction cut-off of ≤ 0.05
588 applied.

589

590 **Acknowledgments**

591 We thank Celeste Romero for help with RNAi experiments, Dr. Kelly Ross for
592 helpful discussions and feedback on the manuscript, and Catherine May from Boston
593 Children's Hospital for helping to set up the RNA-seq analysis and providing template R
594 scripts. J.M.A was supported by the ARCS Fellowship from the ARCS Foundation. This
595 work was supported by NIH R35GM142679 to E.M.D. and NSF IOS-1350302 and NIH
596 R01GM135657 to R.M.Z.

597

598 **Author Contributions**

599 J.M.A. and R.M.Z. conceptualized the study and designed experiments. J.M.A., M.B.,
600 E.B., C.C.M., S.A.Z., and I.I. conducted experiments. J.M.A. and R.M.Z. wrote the
601 original draft of the manuscript. The manuscript was reviewed and edited by J.M.A.,
602 E.M.D., and R.M.Z. Funding for the project was acquired by R.M.Z.

603 ## Figure Legends

604 **Figure 1.** RNAi screen of RING/U-Box E3 ubiquitin ligases identifies regulators of stem
605 cells and regeneration. (A) Feeding and amputation schedule of RNAi screen. Worms
606 were fed twice per week for a total of eight feeds and amputated pre-pharyngeally on
607 day 28. (B) Knockdown of the indicated genes displayed phenotypes including ventral
608 curling and lesions (white arrow). Animals are shown after the conclusion of the RNAi
609 feedings and before amputation. (C) Knockdown of indicated genes that demonstrated
610 phenotypes of delayed or absent regeneration after amputation shown by smaller than
611 normal or absent blastemas (white arrow) and missing or faint eyespots (white
612 arrowhead) when compared to *control(RNAi)* worm at the same regeneration time point.
613 Scale bars = 200 μm.

614

615 **Figure 2.** Inhibition of *prpf19* disrupts stem cell function but is not required for stem cell
616 maintenance. (A) WISH to stem cell markers *tgs-1*, *piwi-1* and *h2b*, and early and late
617 epidermal progeny markers *prog-1* and *agat-1*, respectively, in *control(RNAi)* (upper
618 panels) and *prpf19(RNAi)* animals at 14 (middle panels) and 18 (bottom panels) days
619 after first RNAi feeding. (B) Representative image of animals fixed 14 days after first
620 RNAi feeding for *control(RNAi)* (left) or *prpf19(RNAi)* (right) and immunostained for
621 mitotic marker phospho-histone H3. (C) Quantification of phospho-histone $H3^+$ cells per
622 mm^2 of worms fixed at 11, 14, and 18 days after first RNAi feed (N = 17 – 24 per time
623 point). (D) Representative image of animals fixed 14 days after first RNAi feeding for
624 *control(RNAi)* (left) or *prpf19(RNAi)* (right) and processed for TUNEL staining. (E)

625 Quantification of TUNEL$^+$ cells per mm^2 of worms fixed at 11, 14, and 18 days after first
626 RNAi feed (N = 13 – 16 per time point) All data are represented as mean ± SD. *p-value
627 < 0.05, **p-value < 0.001, ***p-value < 0.0001,Student's t-test with Holm-Sidak
628 correction for multiple comparisons. Scale bars = 200 μm.

629

630 **Figure 3.** *prpf19*-associated factors and downstream targets recapitulate *prpf19(RNAi)*
631 phenotypes. (A) Prpf19 acts as an E3 ligase in NTC, interacting with core complex
632 members PLRG1, CDC5l, and SPF27 to modify U4/U6 snRNP subunit PRPF3 with
633 nonproteolytic K63-linked ubiquitin chains. This ubiquityl mark stabilizes the interaction
634 of PRPF3 with U5 snRNP subunit PRPF8 to allow the stable formation of the U4/U6.U5
635 tri-snRNP and the catalytic activity of the spliceosome. (B) Knockdown of indicated NTC
636 core components displaying head regression. (C) Knockdown of NTC core component
637 *spf27* caused a reduced and delayed regenerative response in amputated worms. At 6
638 days post-amputation, *spf27(RNAi)* worms have smaller blastemas compared to
639 *control(RNAi)* worms at the same time point. At day 11 post-amputation, the
640 regenerative response in *control(RNAi)* worms is largely concluded with large blastemas
641 and visible reformed eyespots present in trunk fragments. In comparison, *spf27(RNAi)*
642 worms have smaller blastemas and have not regenerated eyespots. (D) Inhibition of
643 Prpf19 target *prpf3* and ubiquityl-Prpf3 binding factor *prpf8* demonstrate phenotypes like
644 *prpf19(RNAi)* and includes head regression, lesions, and ventral curling. Scale bars =
645 200 μm.

646

647 **Figure 4.** RNAi-mediated inhibition of canonical PRC1 function disrupts pharyngeal
648 patterning and histone ubiquitylation. (A) Composition and function of PRC1. PRC1
649 functions to ubiquitylate histone H2A and compact chromatin to repress gene
650 expression. (B) Western blot analysis showing a reduction in H2Aub1 levels following
651 *rnf2* inhibition across three biological replicates and two experimental time points. (C)
652 RNAi of PRC1 genes *phc* and *cbx* causes phenotypes of a dorsal lesion anterior to the
653 pharynx and mislocalization of the pharynx on the dorsal surface of the worm. (D) WISH
654 to *NB.22.1E* marks marginal adhesive gland cells, mouth opening, and a population of
655 cells at the base of the pharynx and for *laminin,* which marks the pharynx feeding organ
656 in *control(RNAi)* animals (upper panels) and *phc(RNAi)* animals at days 21 (middle
657 panels) and 28 (bottom panels) after the first RNAi treatment. Scale bars = 200 μm.

658

659 **Figure 5.** Loss of PRC1 function causes changes to gene expression levels and spatial
660 patterning. (A) Volcano plot of differentially expressed genes after 28 days of *rnf2* RNAi
661 treatment. (B) WISH analysis of select genes that were differentially expressed by RNA-
662 seq of *rnf2* RNAi treatment. (C) Volcano plot of differentially expressed genes after 28
663 days of *phc* RNAi. (D) WISH analysis of selected genes indicated to be differentially
664 expressed after *phc* RNAi knockdown. The length of time each probe was developed
665 was equal between target RNAi and control RNAi samples. Arrows indicate up- or
666 down-regulated expression measured by RNA-seq. The red arrows highlight regions
667 with changed expression after RNAi in the worm's brain (B) and mouth (D) regions.
668 Arrowheads indicate regions of ectopic gene expression after RNAi treatment. Scale
669 bars = 200 μm.

670 ## Supplemental Figure Legends

671 **Supplemental Figure S1.** (A) WISH expression patterns for genes showing
672 phenotypes in the RNAi screen. All the genes examined were expressed throughout the
673 parenchyma; a subset of genes displayed enriched expression near the cephalic
674 ganglia or the intestine. (B) WISH analysis showing expression patterns of *prpf19*, *rnf2*,
675 and *phc* in untreated controls (right) and irradiated worms (left). Arrows show
676 expression in regions enriched in stem cells in untreated worms that are undetectable in
677 irradiated worms. Scale bars = 200 μm.

678

679 **Supplemental Figure S2.** (A-B) Double fluorescence *in situ* hybridization showing co-
680 expression of *prpf19* (magenta) with marker genes (green) for stem cells (*piwi-1*, *h2b*),
681 early epidermal progeny marker (*prog-1*), and late epidermal progeny marker (*agat-1*).
682 (C) Western blot probed using an anti-ubiquitin antibody for whole worm homogenate
683 protein extracts from *control(RNAi)* or *prp19f(RNAi)* treated animals collected at days
684 11, 14, and 18 of treatment. Scale bars in A-B = 20 μm.

685

686 **Supplemental Figure S3.** (A) WISH to NTC core elements *cdc5l*, *pflg1*, *spf27*, and
687 spliceosomal RNP members *prpf3* and *prpf8*. Scale bars = 200 μm.

688

689 **Supplemental Figure S4.** (A) Western blot analysis shows a reduction in H2Bub1
690 levels following inhibition of *bre1* at days 14, 21, and 28 of RNAi treatment. (B) Western

691 blot analysis shows no reduction in H2Aub1 levels following inhibition of canonical
692 PRC1 genes *ring1*, *cbx*, and *phc* after 21 days of RNAi treatment. (C) WISH analysis
693 showing expression patterns for PRC1 genes *phc* and *cbx*. (D) WISH marker gene
694 analysis for dorsoventral marker *bmp4* and anterior-posterior marker *ndl-3* showing no
695 change in expression domains following *phc* inhibition. Scale bars = 200 μm.

696

697 **Supplemental Figure S5.** (A) Feeding and sampling schedule for RNA-seq
698 experiments. Worms were fed twice a week and sampled for RNA extraction at the days
699 indicated by the red arrowheads. (B) Volcano plot of differentially expressed genes after
700 28 days of *rnf2* RNAi treatment. (C) Venn diagram showing the overlap between day 28
701 and day 14 sample sets for *rnf2(RNAi)*. (D) GO analysis of down-regulated genes in
702 *rnf2(RNAi)* worms after 28 days of treatment. (E) GO analysis of up-regulated genes in
703 *rnf2(RNAi)* worms after 28 days of treatment.

704 **Table 1: RING/U-box E3 ubiquitin ligases showing phenotypes following RNAi.**

Gene Name	Dresden Contig ID	Human RING or U-box Homolog	E-value	Phenotypes Observed
Smed-bre1	dd_Smed_v6_4070_0_1	RNF40	1e-88	HR, DR
Smed-march5	dd_Smed_v6_4602_0_1	MARCH5	8e-93	HR, Lesions, Lysis
Smed-*not4*	dd_Smed_v6_4767_0_1	CNOT4	5e-87	HR, VC
Smed-prpf19	dd_Smed_v6_1276_0_1	PRPF19	0.0	HR, VC, Lysis
Smed-ran	dd_Smed_v6_330_0_1	CBLB*	3e-94	Lesions, Lysis
Smed-ring1	dd_Smed_v6_12141_0_1	RING1	6e-33	DR
Smed-rnf2	dd_Smed_v6_8989_0_1	RNF2	6e-46	DR
Smed-rnf8-like	dd_Smed_v6_1137_0_5	RNF8	4e-05	DR, Lesions
Smed-traf2-like	dd_Smed_v6_3837_0_1	TRAF2	2e-69	HR

705

706 HR: Head regression. VC: Ventral Curling. DR: Delayed regeneration; *Top Human BLAST hit:
707 RAN, e-value: 9e-116

708

References

1 Elliott, S. A. & Sánchez Alvarado, A. The history and enduring contributions of planarians to the study of animal regeneration. *Wiley Interdiscip Rev Dev Biol* **2**, 301-326, doi:10.1002/wdev.82 (2013).

2 Ivankovic, M. *et al.* Model systems for regeneration: planarians. *Development* **146**, dev167684, doi:10.1242/dev.167684 (2019).

3 Baguñà, J., Saló, E. & Auladell, C. Regeneration and pattern formation in planarians. III. Evidence that neoblasts are totipotent stem cells and the source of blastema cells. *Development* **107**, 77- 86 (1989).

4 Wagner, D. E., Wang, I. E. & Reddien, P. W. Clonogenic neoblasts are pluripotent adult stem cells that underlie planarian regeneration. *Science* **332**, 811-816, doi:10.1126/science.1203983 (2011).

5 Saló, E. & Baguñà, J. Cell movement in intact and regenerating planarians. Quantitation using chromosomal, nuclear and cytoplasmic markers. *Development* **89**, 57-70, doi:10.1242/dev.89.1.57 (1985).

6 Abnave, P. *et al.* Epithelial-mesenchymal transition transcription factors control pluripotent adult stem cell migration in vivo in planarians. *Development* **144**, 3440-3453, doi:10.1242/dev.154971 (2017).

7 Reddien, P. W. The Cellular and Molecular Basis for Planarian Regeneration. *Cell* **175**, 327-345, doi:10.1016/j.cell.2018.09.021 (2018).

8 Labbe, R. M. *et al.* A comparative transcriptomic analysis reveals conserved features of stem cell pluripotency in planarians and mammals. *Stem Cells* **30**, 1734-1745, doi:10.1002/stem.1144 (2012).

9 Onal, P. *et al.* Gene expression of pluripotency determinants is conserved between mammalian and planarian stem cells. *EMBO J* **31**, 2755-2769, doi:10.1038/emboj.2012.110 (2012).

10 van Wolfswinkel, J. C., Wagner, D. E. & Reddien, P. W. Single-cell analysis reveals functionally distinct classes within the planarian stem cell compartment. *Cell Stem Cell* **15**, 326-339, doi:10.1016/j.stem.2014.06.007 (2014).

11 Fincher, C. T., Wurtzel, O., de Hoog, T., Kravarik, K. M. & Reddien, P. W. Cell type transcriptome atlas for the planarian Schmidtea mediterranea. *Science* **360**, doi:10.1126/science.aaq1736 (2018).

12 Plass, M. *et al.* Cell type atlas and lineage tree of a whole complex animal by single-cell transcriptomics. *Science*, doi:10.1126/science.aaq1723 (2018) (2018).

13 Boser, A. *et al.* SILAC proteomics of planarians identifies Ncoa5 as a conserved component of pluripotent stem cells. *Cell Rep* **5**, 1142-1155, doi:10.1016/j.celrep.2013.10.035 (2013).

746 14 Fernandez-Taboada, E., Rodriguez-Esteban, G., Salo, E. & Abril, J. F. A proteomics
747 approach to decipher the molecular nature of planarian stem cells. *BMC Genomics* **12**,
748 133, doi:10.1186/1471-2164-12-133 (2011).

749 15 Strand, N. S. *et al.* Dissecting the function of Cullin-RING ubiquitin ligase complex genes
750 in planarian regeneration. *Dev Biol* **433**, 210-217, doi:10.1016/j.ydbio.2017.10.011
751 (2018).

752 16 Ciechanover, A., Finley, D. & Varshavsky, A. Ubiquitin dependence of selective protein
753 degradation demonstrated in the mammalian cell cycle mutant ts85. *Cell* **37**, 57-66,
754 doi:10.1016/0092-8674(84)90300-3 (1984).

755 17 Endoh, M. *et al.* Histone H2A mono-ubiquitination is a crucial step to mediate PRC1-
756 dependent repression of developmental genes to maintain ES cell identity. *PLoS Genet*
757 **8**, e1002774, doi:10.1371/journal.pgen.1002774 (2012).

758 18 Higgins, R. *et al.* The Unfolded Protein Response Triggers Site-Specific Regulatory
759 Ubiquitylation of 40S Ribosomal Proteins. *Mol Cell* **59**, 35-49,
760 doi:10.1016/j.molcel.2015.04.026 (2015).

761 19 Nakayama, K. I. & Nakayama, K. Regulation of the cell cycle by SCF-type ubiquitin
762 ligases. *Semin Cell Dev Biol* **16**, 323-333, doi:10.1016/j.semcdb.2005.02.010 (2005).

763 20 Werner, A., Manford, A. G. & Rape, M. Ubiquitin-Dependent Regulation of Stem Cell
764 Biology. *Trends Cell Biol* **27**, 568-579, doi:10.1016/j.tcb.2017.04.002 (2017).

765 21 Li, W. *et al.* Genome-wide and functional annotation of human E3 ubiquitin ligases
766 identifies MULAN, a mitochondrial E3 that regulates the organelle's dynamics and
767 signaling. *PLoS One* **3**, e1487, doi:10.1371/journal.pone.0001487 (2008).

768 22 Lorick, K. L. *et al.* RING fingers mediate ubiquitin-conjugating enzyme (E2)-dependent
769 ubiquitination. *Proc Natl Acad Sci U S A* **96**, 11364-11369,
770 doi:10.1073/pnas.96.20.11364 (1999).

771 23 Aravind, L. & Koonin, E. V. The U box is a modified RING finger - a common domain in
772 ubiquitination. *Curr Biol* **10**, 132-134, doi:http://dx.doi.org/10.1016/S0960-
773 9822(00)00398-5 (2000).

774 24 Henderson, J. M. *et al.* Identification of HECT E3 ubiquitin ligase family genes involved
775 in stem cell regulation and regeneration in planarians. *Dev Biol* **404**, 21-34,
776 doi:10.1016/j.ydbio.2015.04.021 (2015).

777 25 Brandl, H. *et al.* PlanMine--a mineable resource of planarian biology and biodiversity.
778 *Nucleic Acids Res* **44**, D764-773, doi:10.1093/nar/gkv1148 (2016).

779 26 Roberts-Galbraith, R. H., Brubacher, J. L. & Newmark, P. A. A functional genomics
780 screen in planarians reveals regulators of whole-brain regeneration. *Elife* **5**,
781 doi:10.7554/eLife.17002 (2016).

782 27 Eisenhoffer, G. T., Kang, H. & Sánchez Alvarado, A. Molecular analysis of stem cells
783 and their descendants during cell turnover and regeneration in the planarian Schmidtea
784 mediterranea. *Cell Stem Cell* **3**, 327-339, doi:10.1016/j.stem.2008.07.002 (2008).

785 28 Lu, X. & Legerski, R. J. The Prp19/Pso4 core complex undergoes ubiquitylation and
786 structural alterations in response to DNA damage. *Biochem Biophys Res Commun* **354**,
787 968-974, doi:10.1016/j.bbrc.2007.01.097 (2007).

788 29 Hwang, W. W. *et al.* A Conserved RING Finger Protein Required for Histone H2B
789 Monoubiquitination and Cell Size Control. *Molecular Cell* **11**, 261-266,
790 doi:10.1016/s1097-2765(02)00826-2 (2003).

791 30 Henry, K. W. *et al.* Transcriptional activation via sequential histone H2B ubiquitylation
792 and deubiquitylation, mediated by SAGA-associated Ubp8. *Genes Dev* **17**, 2648-2663,
793 doi:10.1101/gad.1144003 (2003).

794 31 Wang, H. *et al.* Role of histone H2A ubiquitination in Polycomb silencing. *Nature* **431**,
795 873-878, doi:10.1038/nature02985 (2004).

796 32 Bunker, C. A. & Kingston, R. E. Transcriptional repression by Drosophila and
797 mammalian Polycomb group proteins in transfected mammalian cells. *Mol Cell Biol* **14**,
798 1721-1732, doi:10.1128/mcb.14.3.1721-1732.1994 (1994).

799 33 de Napoles, M. *et al.* Polycomb group proteins Ring1A/B link ubiquitylation of histone
800 H2A to heritable gene silencing and X inactivation. *Dev Cell* **7**, 663-676,
801 doi:10.1016/j.devcel.2004.10.005 (2004).

802 34 Gao, Z. *et al.* PCGF homologs, CBX proteins, and RYBP define functionally distinct
803 PRC1 family complexes. *Mol Cell* **45**, 344-356, doi:10.1016/j.molcel.2012.01.002 (2012).

804 35 Fursova, N. A. *et al.* Synergy between Variant PRC1 Complexes Defines Polycomb-
805 Mediated Gene Repression. *Mol Cell* **74**, 1020-1036 e1028,
806 doi:10.1016/j.molcel.2019.03.024 (2019).

807 36 Gavino, M. A. & Reddien, P. W. A Bmp/Admp regulatory circuit controls maintenance
808 and regeneration of dorsal-ventral polarity in planarians. *Curr Biol* **21**, 294-299,
809 doi:10.1016/j.cub.2011.01.017 (2011).

810 37 Rink, J. C., Gurley, K. A., Elliott, S. A. & Sánchez Alvarado, A. Planarian Hh signaling
811 regulates regeneration polarity and links Hh pathway evolution to cilia. *Science* **326**,
812 1406-1410, doi:10.1126/science.1178712 (2009).

813 38 Adler, C. E., Seidel, C. W., McKinney, S. A. & Sánchez Alvarado, A. Selective
814 amputation of the pharynx identifies a FoxA-dependent regeneration program in
815 planaria. *Elife* **3**, e02238, doi:10.7554/eLife.02238 (2014).

816 39 Tu, K. C. *et al.* Egr-5 is a post-mitotic regulator of planarian epidermal differentiation.
817 *Elife* **4**, e10501, doi:10.7554/eLife.10501 (2015).

818 40 Song, E. J. *et al.* The Prp19 complex and the Usp4Sart3 deubiquitinating enzyme control
819 reversible ubiquitination at the spliceosome. *Genes Dev* **24**, 1434-1447,
820 doi:10.1101/gad.1925010 (2010).

821 41 Reddien, P. W., Oviedo, N. J., Jennings, J. R., Jenkin, J. C. & Sánchez Alvarado, A.
822 SMEDWI-2 is a PIWI-like protein that regulates planarian stem cells. *Science* **310**, 1327-
823 1330, doi:10.1126/science.1116110 (2005).

824 42 Kim, I. V. *et al.* Planarians recruit piRNAs for mRNA turnover in adult stem cells. *Genes*
825 *Dev* **33**, 1575-1590, doi:10.1101/gad.322776.118 (2019).

826 43 Rouhana, L., Shibata, N., Nishimura, O. & Agata, K. Different requirements for
827 conserved post-transcriptional regulators in planarian regeneration and stem cell
828 maintenance. *Dev Biol* **341**, 429-443, doi:10.1016/j.ydbio.2010.02.037 (2010).

829 44 Solana, J. *et al.* The CCR4-NOT complex mediates deadenylation and degradation of
830 stem cell mRNAs and promotes planarian stem cell differentiation. *PLoS Genet* **9**,
831 e1004003, doi:10.1371/journal.pgen.1004003 (2013).

832 45 Francis, N. J., Kingston, R. E. & Woodcock, C. L. Chromatin compaction by a polycomb
833 group protein complex. *Science* **306**, 1574-1577, doi:10.1126/science.1100576 (2004).

834 46 Shao, Z. *et al.* Stabilization of Chromatin Structure by PRC1, a Polycomb Complex. *Cell*
835 **98**, 37-46, doi:10.1016/s0092-8674(00)80604-2 (1999).

836 47 Tamburri, S. *et al.* Histone H2AK119 Mono-Ubiquitination Is Essential for Polycomb-
837 Mediated Transcriptional Repression. *Mol Cell*, doi:10.1016/j.molcel.2019.11.021 (2019).

838 48 Blackledge, N. P. *et al.* PRC1 Catalytic Activity Is Central to Polycomb System Function.
839 *Mol Cell* **77**, 857-874 e859, doi:10.1016/j.molcel.2019.12.001 (2020).

840 49 Pengelly, A. R., Kalb, R., Finkl, K. & Muller, J. Transcriptional repression by PRC1 in the
841 absence of H2A monoubiquitylation. *Genes Dev* **29**, 1487-1492,
842 doi:10.1101/gad.265439.115 (2015).

843 50 Lewis, E. B. A gene complex controlling segmentation in Drosophila. *Nature* **276**, 565-
844 570, doi:10.1038/276565a0 (1978).

845 51 Conway, E. M. & Bracken, A. P. in *Polycomb Group Proteins* 57-80 (2017).

846 52 Cao, R., Tsukada, Y. & Zhang, Y. Role of Bmi-1 and Ring1A in H2A ubiquitylation and
847 Hox gene silencing. *Mol Cell* **20**, 845-854, doi:10.1016/j.molcel.2005.12.002 (2005).

848 53 Blackledge, N. P. *et al.* Variant PRC1 complex-dependent H2A ubiquitylation drives
849 PRC2 recruitment and polycomb domain formation. *Cell* **157**, 1445-1459,
850 doi:10.1016/j.cell.2014.05.004 (2014).

851 54 Gahan, J. M., Rentzsch, F. & Schnitzler, C. E. The genetic basis for PRC1 complex
852 diversity emerged early in animal evolution. *Proc Natl Acad Sci U S A*,
853 doi:10.1073/pnas.2005136117 (2020).

854 55 Peng, Y. C., Lv, T. H., Du, Z. K., Cun, X. N. & Yang, K. M. Liver Macrophages Stimulate
855 the Expression of Hepatocyte Nuclear Factor-6 and Promote Hepatocyte Proliferation at
856 the Early Stage of Liver Regeneration. *Bull Exp Biol Med* **170**, 40-45,
857 doi:10.1007/s10517-020-05000-7 (2020).

858 56 van der Raadt, J., van Gestel, S. H. C., Nadif Kasri, N. & Albers, C. A. ONECUT
859 transcription factors induce neuronal characteristics and remodel chromatin accessibility.
860 *Nucleic Acids Res* **47**, 5587-5602, doi:10.1093/nar/gkz273 (2019).

861 57 Jiang, K. *et al.* HNF6 promotes tumor growth in colorectal cancer and enhances liver
862 metastasis in mouse model. *J Cell Physiol* **234**, 3675-3684, doi:10.1002/jcp.27140
863 (2019).

864 58 Lee, T. I., Johnstone, S. E. & Young, R. A. Chromatin immunoprecipitation and
865 microarray-based analysis of protein location. *Nat Protoc* **1**, 729-748,
866 doi:10.1038/nprot.2006.98 (2006).

867 59 Skene, P. J. & Henikoff, S. An efficient targeted nuclease strategy for high-resolution
868 mapping of DNA binding sites. *Elife* **6**, doi:10.7554/eLife.21856 (2017).

869 60 Merryman, M. S., Sánchez Alvarado, A. & Jenkin, J. C. Culturing Planarians in the
870 Laboratory. *Methods Mol Biol* **1774**, 241-258, doi:10.1007/978-1-4939-7802-1_5 (2018).

871 61 Rozanski, A. *et al.* PlanMine 3.0-improvements to a mineable resource of flatworm
872 biology and biodiversity. *Nucleic Acids Res* **47**, D812-D820, doi:10.1093/nar/gky1070
873 (2019).

874 62 Blum, M. *et al.* The InterPro protein families and domains database: 20 years on. *Nucleic*
875 *Acids Res* **49**, D344-D354, doi:10.1093/nar/gkaa977 (2021).

876 63 Zayas, R. M. *et al.* The planarian Schmidtea mediterranea as a model for epigenetic
877 germ cell specification: analysis of ESTs from the hermaphroditic strain. *Proc Natl Acad*
878 *Sci U S A* **102**, 18491-18496, doi:10.1073/pnas.0509507102 (2005).

879 64 Liu, S. Y. *et al.* Reactivating head regrowth in a regeneration-deficient planarian species.
880 *Nature* **500**, 81-84, doi:10.1038/nature12414 (2013).

881 65 Adler, C. E. & Sánchez Alvarado, A. Systemic RNA Interference in Planarians by
882 Feeding of dsRNA Containing Bacteria. *Methods Mol Biol* **1774**, 445-454,
883 doi:10.1007/978-1-4939-7802-1_17 (2018).

884 66 Rouhana, L. *et al.* RNA interference by feeding in vitro-synthesized double-stranded
885 RNA to planarians: methodology and dynamics. *Dev Dyn* **242**, 718-730,
886 doi:10.1002/dvdy.23950 (2013).

887 67 Gurley, K. A., Rink, J. C. & Sánchez Alvarado, A. β-Catenin Defines Head Versus Tail
888 Identity During Planarian Regeneration and Homeostasis. *Science* **319**, 323-327 (2008).

889 68 Pearson, B. J. *et al.* Formaldehyde-based whole-mount in situ hybridization method for
890 planarians. *Dev Dyn* **238**, 443-450, doi:10.1002/dvdy.21849 (2009).

891 69 King, R. S. & Newmark, P. A. *In situ* hybridization protocol for enhanced detection of
892 gene expression in the planarian *Schmidtea mediterranea*. *BMC Developmental Biology*
893 **13** (2013).

894 70 Lauter, G., Soll, I. & Hauptmann, G. Two-color fluorescent in situ hybridization in the
895 embryonic zebrafish brain using differential detection systems. *BMC Dev Biol* **11**, 43,
896 doi:10.1186/1471-213X-11-43 (2011).

897 71 Brown, D. D. R. & Pearson, B. J. in *In Situ Hybridization Methods Neuromethods* Ch.
898 Chapter 7, 127-150 (2015).

899 72 Pellettieri, J. *et al.* Cell death and tissue remodeling in planarian regeneration. *Dev Biol*
900 **338**, 76-85, doi:10.1016/j.ydbio.2009.09.015 (2010).

901 73 Simoes, A. E. *et al.* Efficient recovery of proteins from multiple source samples after
902 TRIzol((R)) or TRIzol((R))LS RNA extraction and long-term storage. *BMC Genomics* **14**,
903 181, doi:10.1186/1471-2164-14-181 (2013).

904 74 Duncan, E. M., Chitsazan, A. D., Seidel, C. W. & Sánchez Alvarado, A. Set1 and MLL1/2
905 Target Distinct Sets of Functionally Different Genomic Loci In Vivo. *Cell Rep* **13**, 2741-
906 2755, doi:10.1016/j.celrep.2015.11.059 (2015).

907 75 Bray, N. L., Pimentel, H., Melsted, P. & Pachter, L. Near-optimal probabilistic RNA-seq
908 quantification. *Nat Biotechnol* **34**, 525-527, doi:10.1038/nbt.3519 (2016).

909 76 Huber, W. *et al.* Orchestrating high-throughput genomic analysis with Bioconductor. *Nat*
910 *Methods* **12**, 115-121, doi:10.1038/nmeth.3252 (2015).

911 77 Love, M. I., Huber, W. & Anders, S. Moderated estimation of fold change and dispersion
912 for RNA-seq data with DESeq2. *Genome Biol* **15**, 550, doi:10.1186/s13059-014-0550-8
913 (2014).

914

Figure 1

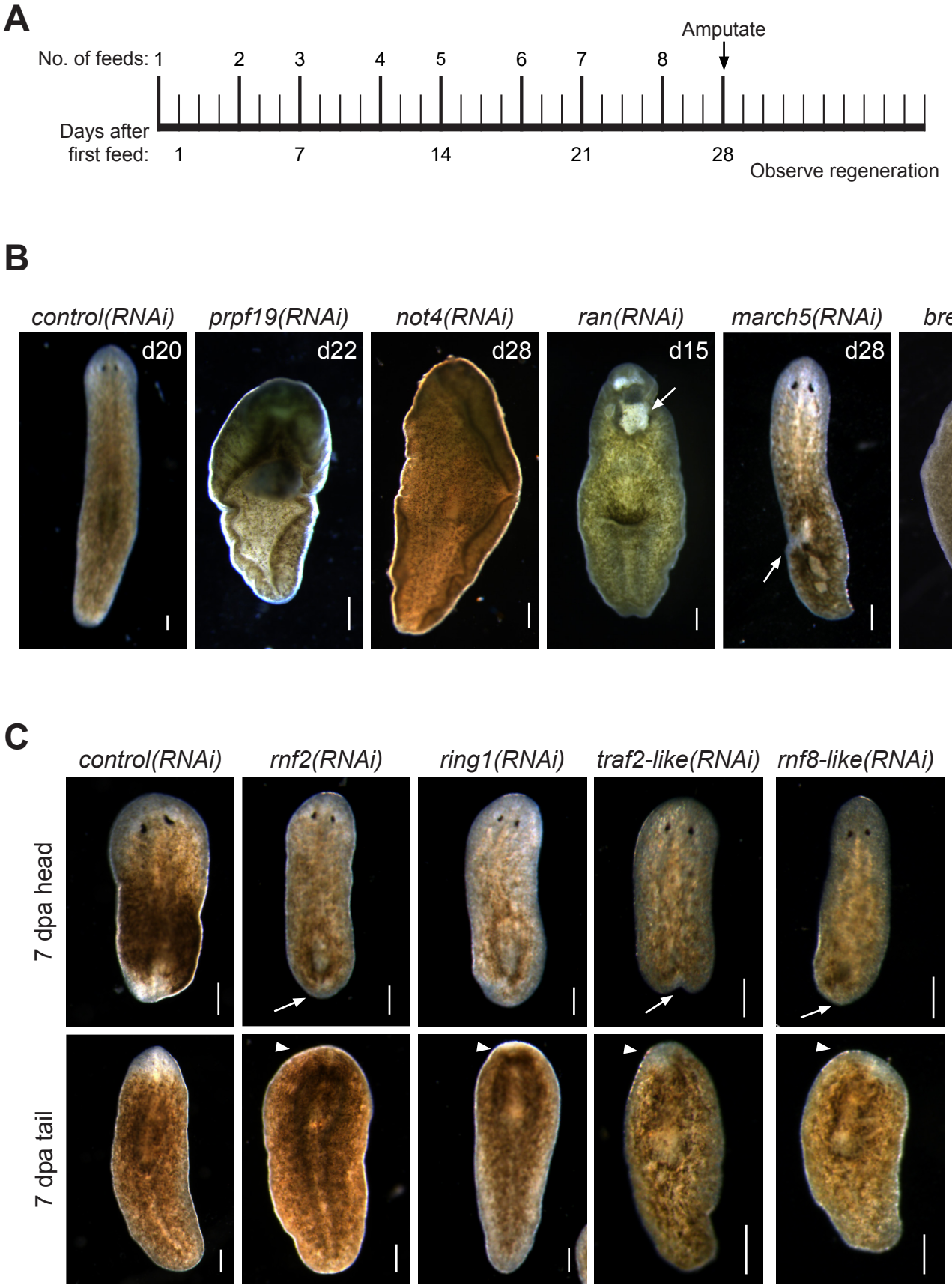
A
Amputate
No. of feeds: 1 2 3 4 5 6 7 8
Days after first feed: 1 7 14 21 28
Observe regeneration
B
control(RNAi)
prpf19(RNAi)
not4(RNAi)
ran(RNAi)
march5(RNAi)
bre1(RNAi)
d20
d22
d28
d15
d28
d21
C
control(RNAi)
rnf2(RNAi)
ring1(RNAi)
traf2-like(RNAi)
rnf8-like(RNAi)
7 dpa head
7 dpa tail

Supplemental Figure S1

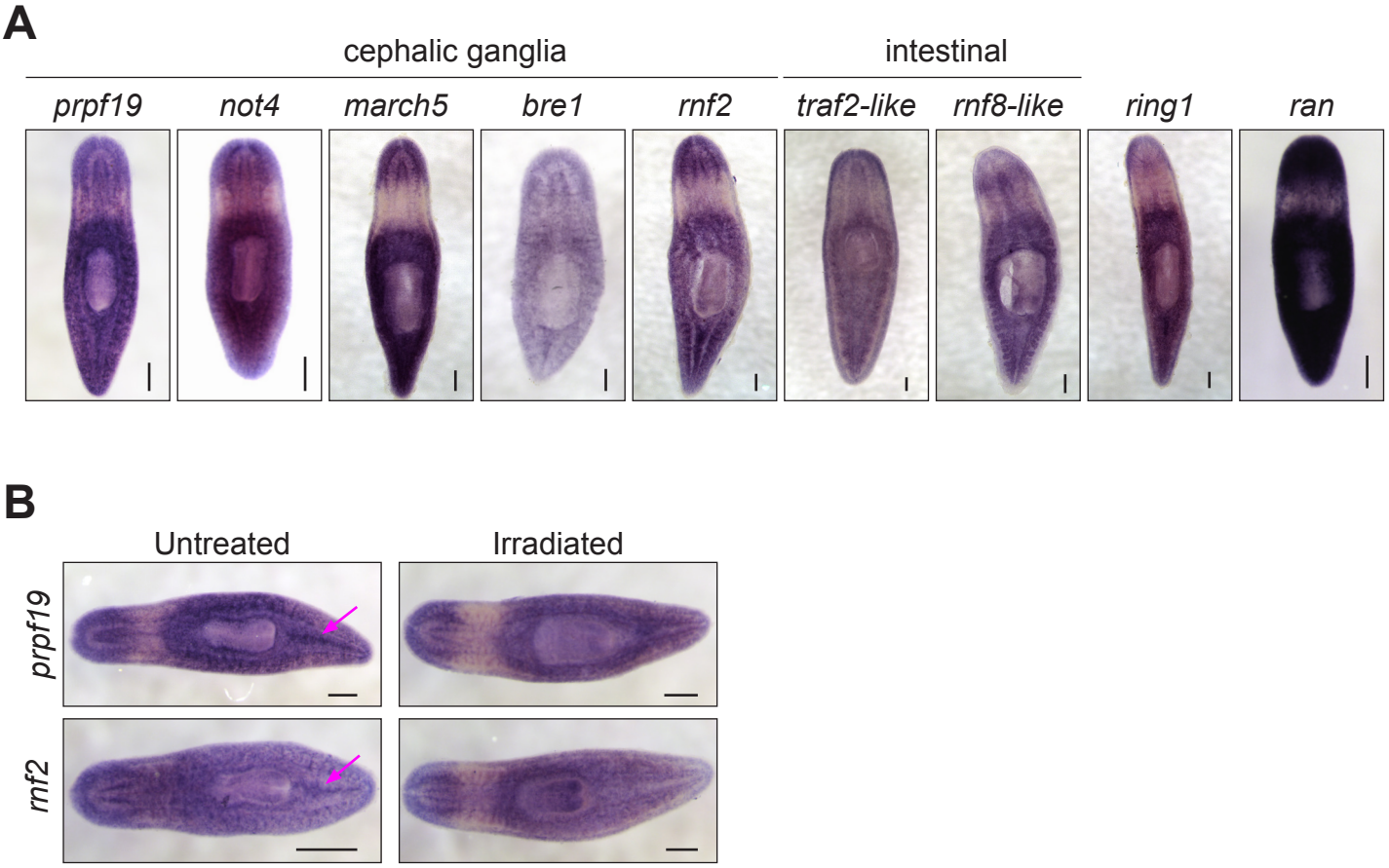

Figure 2

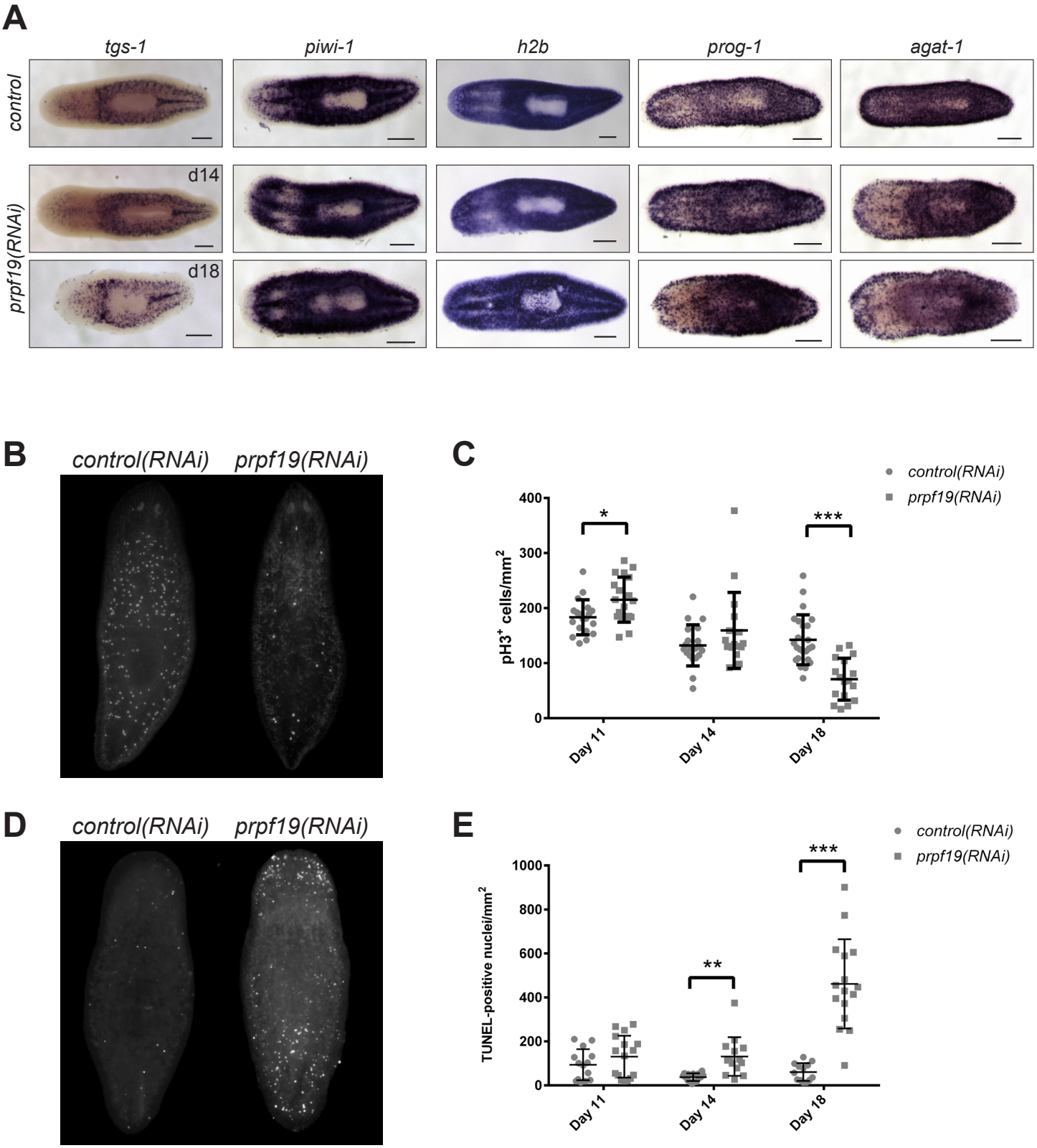
A
tgs-1
piwi-1
h2b
prog-1
agat-1
control
prpf19(RNAi)
d14
d18
B
control(RNAi)
prpf19(RNAi)
C
control(RNAi)
prpf19(RNAi)
pH3+ cells/mm2
400
300
200
100
0
*
***
Day 11
Day 14
Day 18
D
control(RNAi)
prpf19(RNAi)
E
control(RNAi)
prpf19(RNAi)
TUNEL-positive nuclei/mm2
1000
800
600
400
200
0
***
**
Day 11
Day 14
Day 18

Supplemental Figure S2

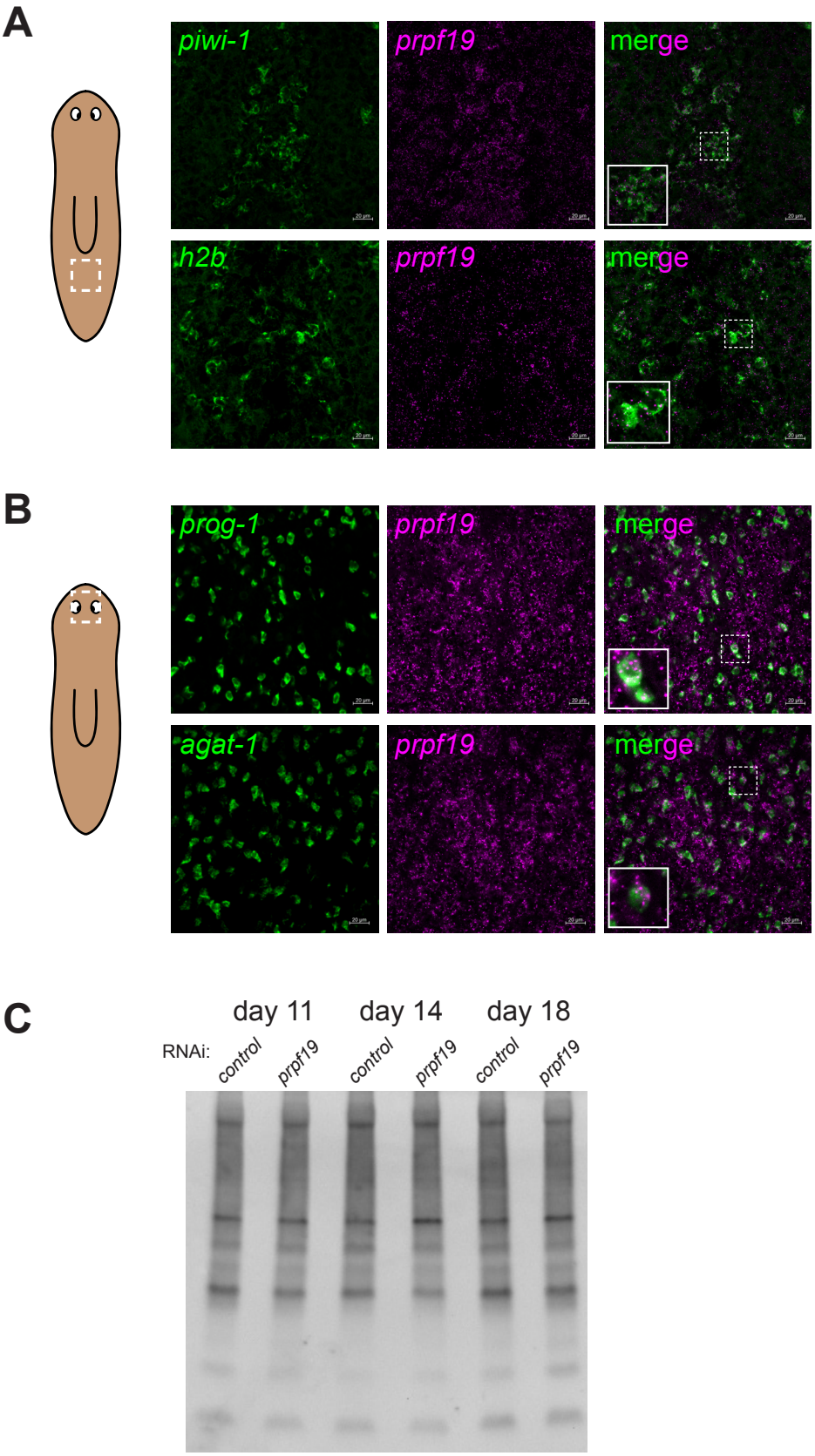

Figure 3

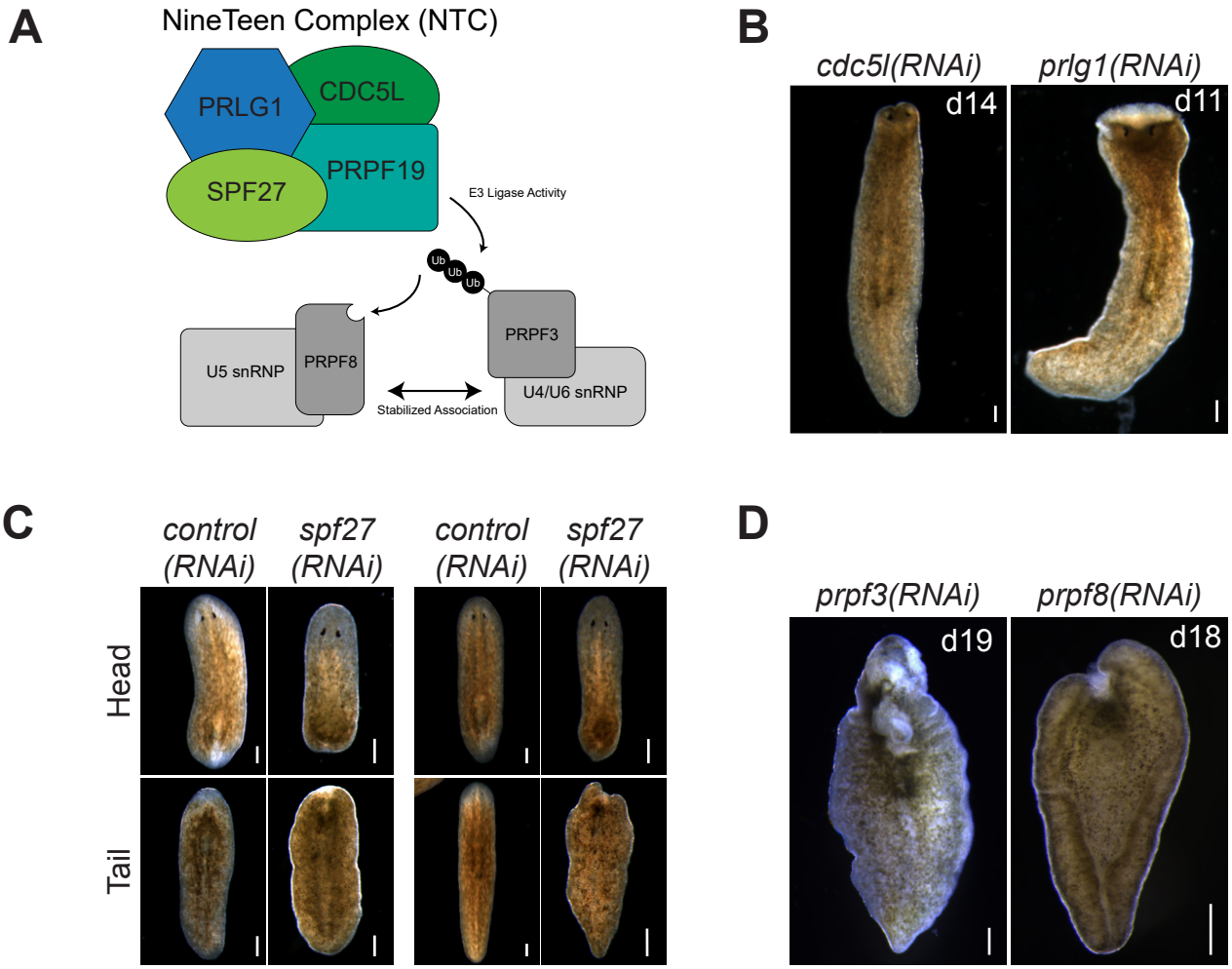
A
NineTeen Complex (NTC)
PRLG1
CDC5L
PRPF19
SPF27
E3 Ligase Activity
Ub
Ub
Ub
PRPF3
U5 snRNP
PRPF8
U4/U6 snRNP
Stabilized Association
B
cdc5l(RNAi)
prlg1(RNAi)
d14
d11
C
control (RNAi)
spf27 (RNAi)
control (RNAi)
spf27 (RNAi)
Head
Tail
D
prpf3(RNAi)
prpf8(RNAi)
d19
d18

Supplemental Figure S3

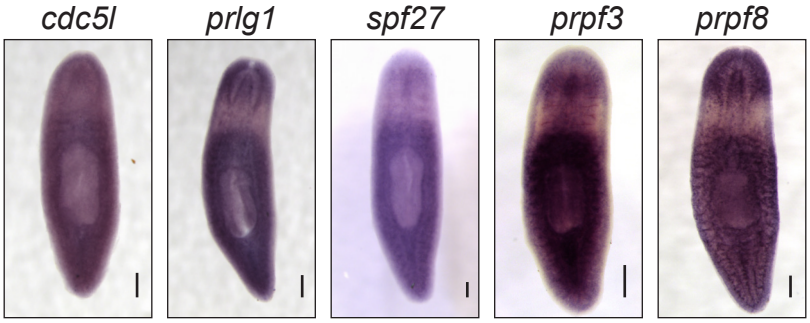

Figure 4

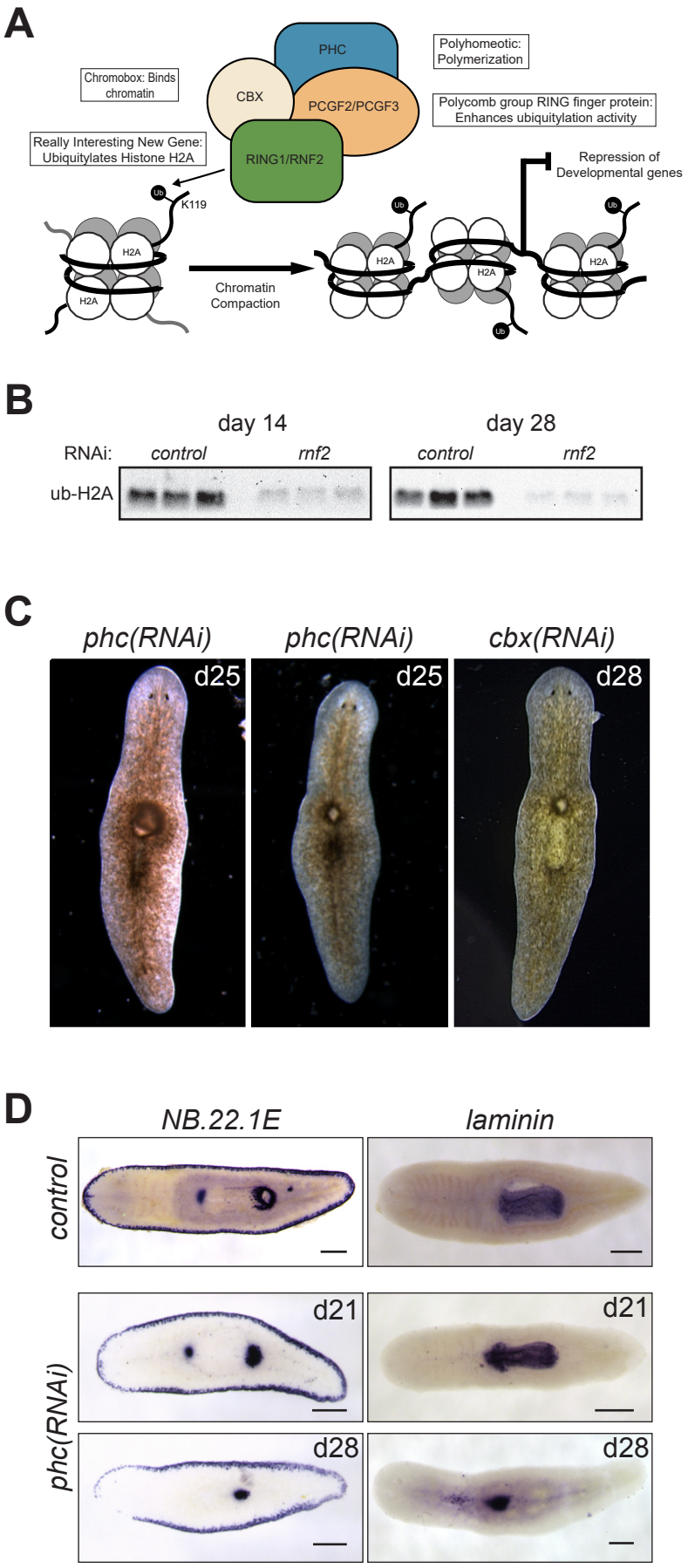
A
PHC
CBX
PCGF2/PCGF3
RING1/RNF2
Chromobox: Binds chromatin
Polyhomeotic: Polymerization
Polycomb group RING finger protein: Enhances ubiquitylation activity
Really Interesting New Gene: Ubiquitylates Histone H2A
Repression of Developmental genes
Ub
K119
H2A
Chromatin Compaction
B
day 14
day 28
RNAi:
control
rnf2
control
rnf2
ub-H2A
C
phc(RNAi)
phc(RNAi)
cbx(RNAi)
d25
d25
d28
D
NB.22.1E
laminin
control
phc(RNAi)
d21
d21
d28
d28

Supplemental Figure S4

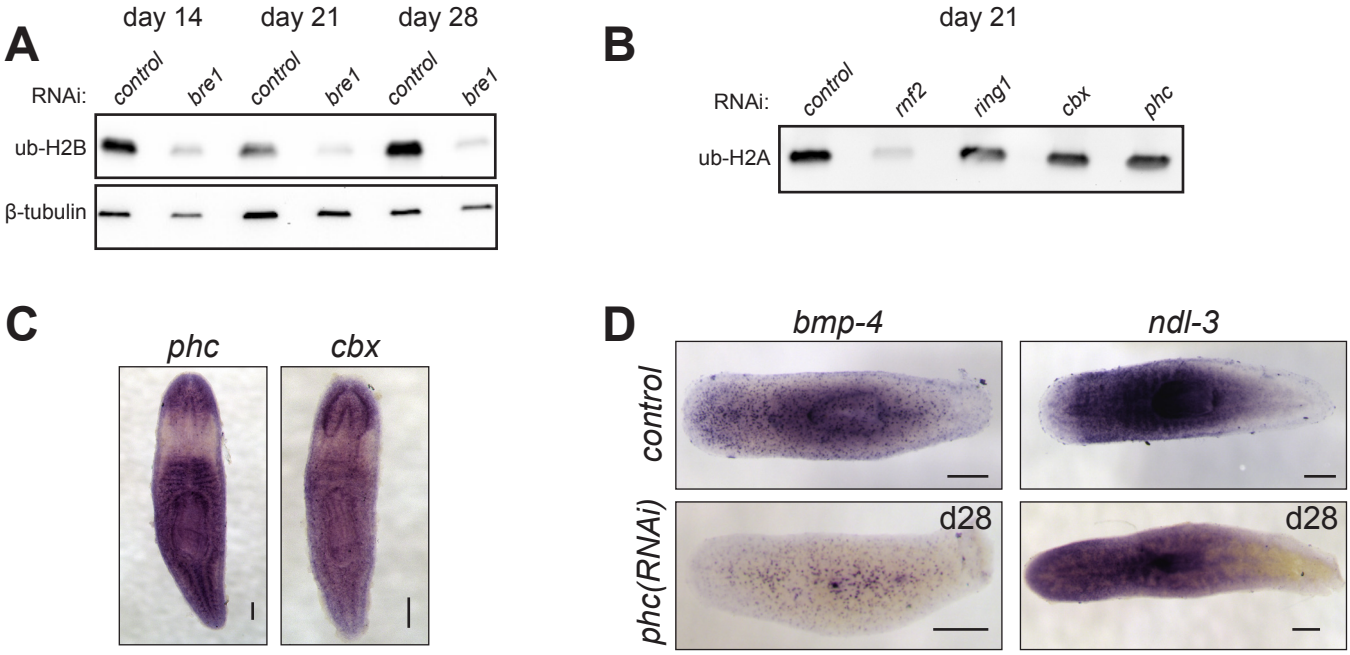

Figure 5

A

Total number of differentially expressed genes identified by RNA-seq at FDR value < 0.1.

Gene name	Days of RNAi	Down-regulated genes	Up-regulated genes	Total
Smed-phc	11	20	29	49
Smed-rnf2	14	16	13	29
Smed-rnf2	28	113	134	247

B

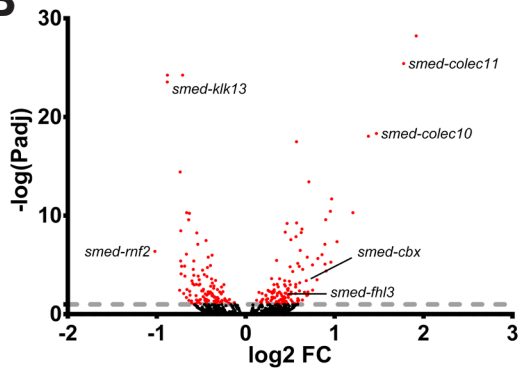

C

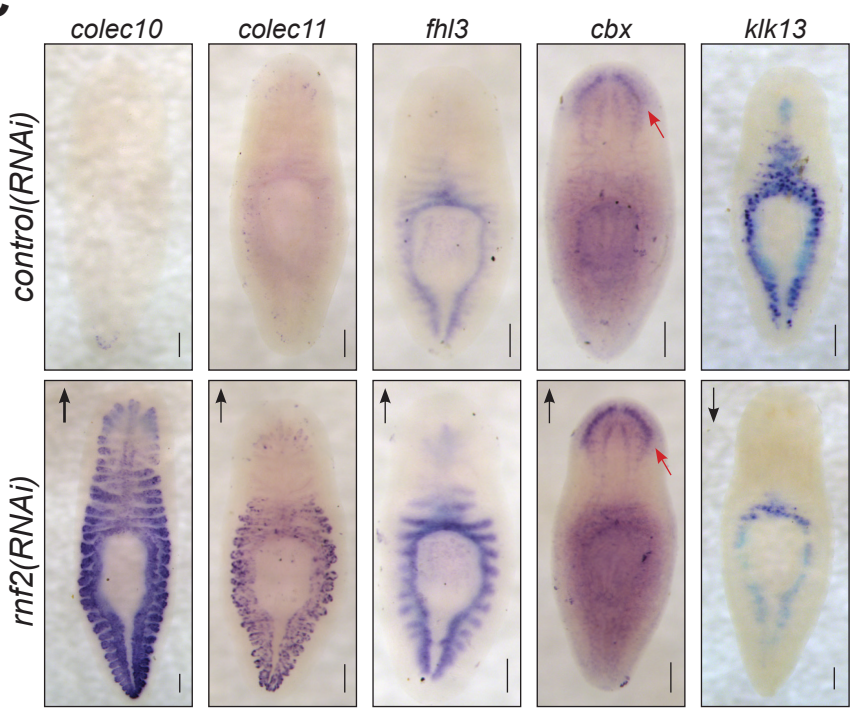

D

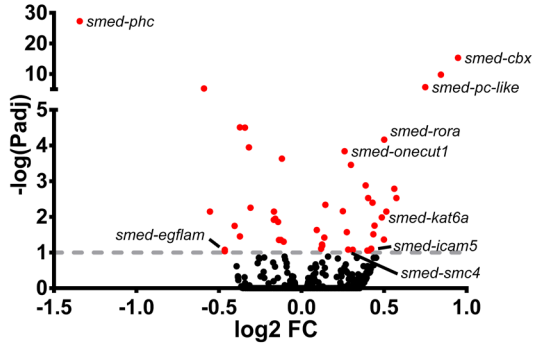

E

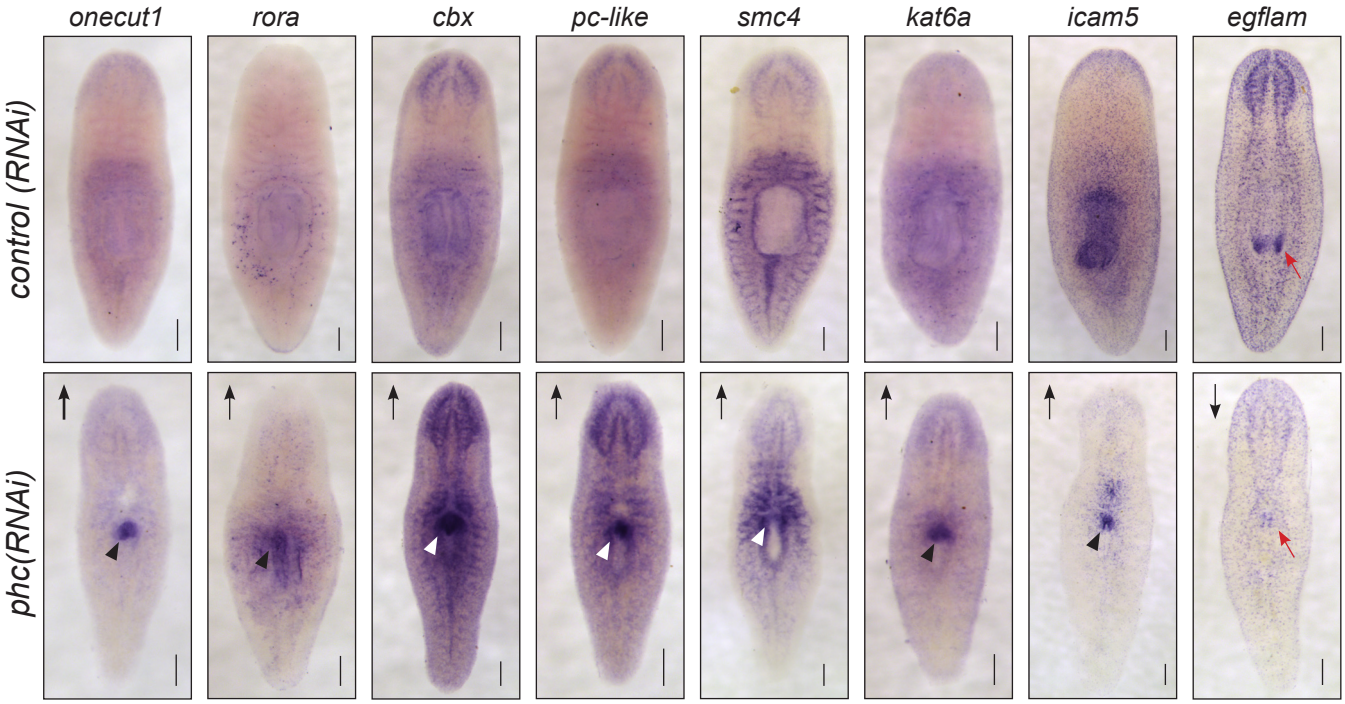
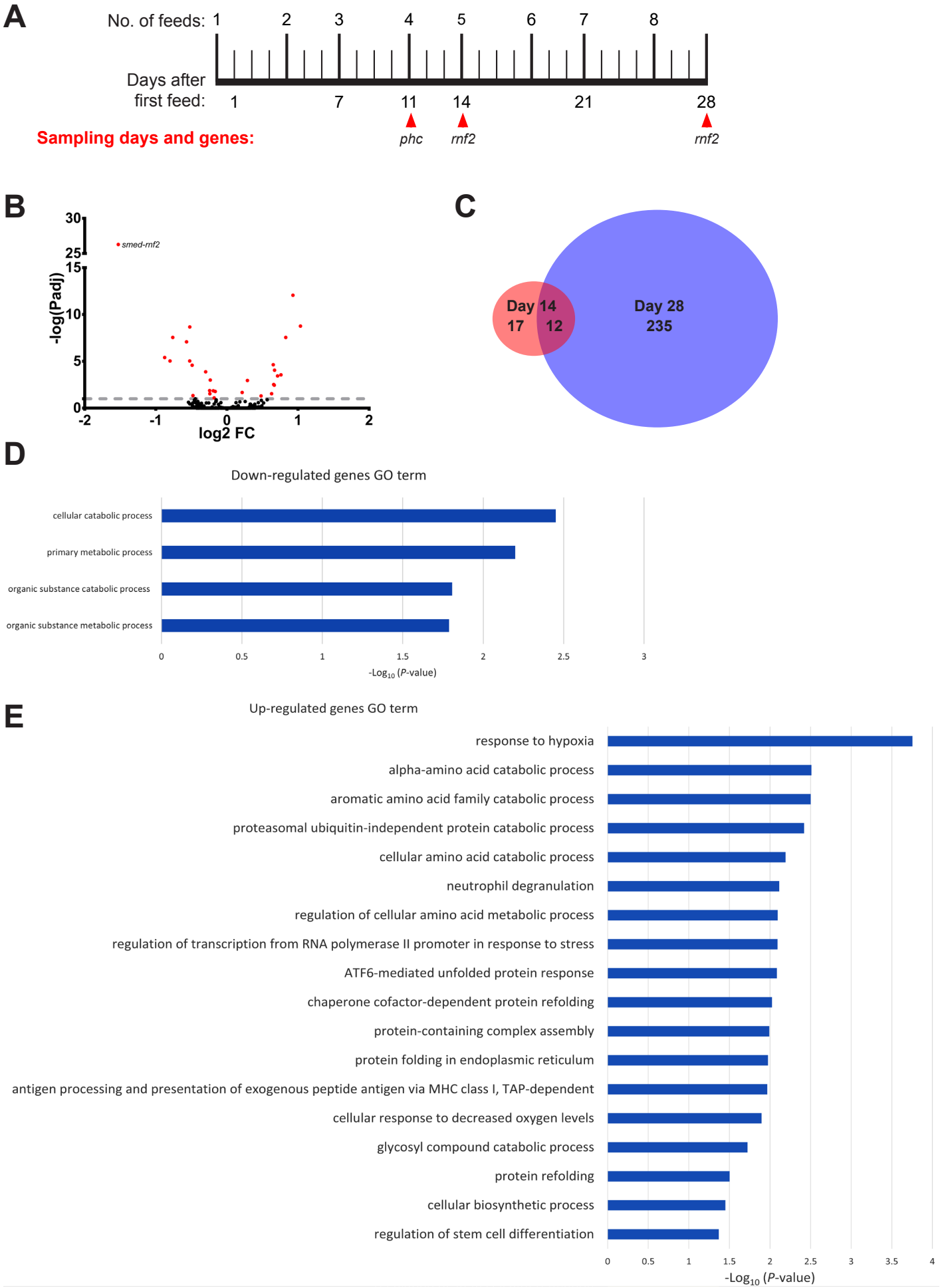
Supplemental Figure S5